UNIVERSIDADE DE SÃO PAULO
Instituto de Ciências Matemáticas e de Computação

Linear Stability Theory Applied to Three-Dimensional Viscoelastic Fluid Flows

Laison Junio da Silva Furlan

Tese de Doutorado do Programa de Pós-Graduação em Ciências de Computação e Matemática Computacional (PPG-CCMC)

ICMC USP
SÃO CARLOS

Laison Junio da Silva Furlan

Linear Stability Theory Applied to Three-Dimensional Viscoelastic Fluid Flows

Doctoral dissertation submitted to the Instituto de Ciências Matemáticas e de Computação – ICMC-USP, in partial fulfillment of the requirements for the degree of the Doctorate Program in Computer Science and Computational Mathematics. *FINAL VERSION*

Concentration Area: Computer Science and Computational Mathematics

Advisor: Prof. Dr. Leandro Franco de Souza

USP – São Carlos
November 2022

Ficha catalográfica elaborada pela Biblioteca Prof. Achille Bassi
e Seção Técnica de Informática, ICMC/USP,
com os dados inseridos pelo(a) autor(a)

Furlan, Laison Junio da Silva
F985l Linear Stability Theory Applied to Three-Dimensional Viscoelastic Fluid Flows / Laison Junio da Silva Furlan; orientador Leandro Franco de Souza. -- São Carlos, 2022.
87 p.

Tese (Doutorado - Programa de Pós-Graduação em Ciências de Computação e Matemática Computacional) -- Instituto de Ciências Matemáticas e de Computação, Universidade de São Paulo, 2022.

1. Linear Stability Theory. 2. UCM Model. 3. Oldroyd-B Model. 4. Giesekus Model. 5. LPTT Model. I. Souza, Leandro Franco de, orient. II. Título.

Bibliotecários responsáveis pela estrutura de catalogação da publicação de acordo com a AACR2:
Gláucia Maria Saia Cristianini - CRB - 8/4938
Juliana de Souza Moraes - CRB - 8/6176

Laison Junio da Silva Furlan

Teoria de Estabilidade Linear Aplicada a Escoamentos Tridimensionais de Fluidos Viscoelásticos

Tese apresentada ao Instituto de Ciências Matemáticas e de Computação – ICMC-USP, como parte dos requisitos para obtenção do título de Doutor em Ciências – Ciências de Computação e Matemática Computacional. *VERSÃO REVISADA*

Área de Concentração: Ciências de Computação e Matemática Computacional

Orientador: Prof. Dr. Leandro Franco de Souza

USP – São Carlos
Novembro de 2022

To my parents, my girlfriend and friends.

ACKNOWLEDGEMENTS

Agradeço, primeiramente, a minha família, meu pai José Roberto, minha mãe Lídia, meu irmão Dexter e a minha namorada Larah, pois sempre me apoiaram e me motivaram nesta minha jornada acadêmica.

Ao meu orientador, professor Leandro Franco de Souza, pelo apoio e ensinamentos, e também pelo companheirismo e amizade, contribuindo não apenas para a elaboração deste trabalho mas também para a minha formação pessoal.

Ao professor Márcio T. Mendonça, pelo apoio e auxílio no desenvolvimento dessa pesquisa. Sem a sua ajuda, certamente este trabalho não seria plenamente desenvolvido. Ao professor André Cavalieri, pelas considerações feitas durante o meu exame de qualificação, considerações essas que foram fundamentais para o avanço e conclusão deste trabalho.

Aos professores do departamento de Matemática e Computação da FCT-UNESP, em especial a professora Analice Costacurta Brandi, pela orientação acadêmica, pela amizade e o compartilhamento dos conhecimentos e experiências.

Aos meus amigos do LMACC, em especial Matheus Tozo, amigos esses que fiz no dia a dia, dividindo não só o laboratório como também experiências de vida e momentos felizes. Ao funcionário do laboratório LMACC, Leonardo José Martinussi, pelo companheirismo, eficiência e prontidão para sempre ajudar os alunos no que fosse preciso, bem como no uso do cluster Euler. Sem o seu apoio, certamente esta pesquisa enfrentaria maiores dificuldades além das que foram enfrentadas.

Aos amigos que fiz na minha vinda para São Carlos, aos amigos que ficaram em Presidente Prudente, e aos amigos que a vida levou para outros caminhos.

O presente trabalho foi realizado com apoio da Coordenação de Aperfeiçoamento de Pessoal de Nível Superior - Brasil (CAPES) - Código de Financiamento 001.

À Universidade de São Paulo (USP), ao Instituto de Ciências Matemáticas e de Computação (ICMC), ao Centro de Matemática Aplicada à Indústria (CeMEAI) financiado pela FAPESP (Número do Processo: 2013/070375-0), aos professores deste instituto, e a todos que contribuíram para a realização desta pesquisa, de forma direta ou indireta.

“I was never aware of any other option
but to question everything.”
(Noam Chomsky)

RESUMO

FURLAN, L. J. S. **Teoria de Estabilidade Linear Aplicada a Escoamentos Tridimensionais de Fluidos Viscoelásticos**. 2022. 86 p. Tese (Doutorado em Ciências – Ciências de Computação e Matemática Computacional) – Instituto de Ciências Matemáticas e de Computação, Universidade de São Paulo, São Carlos – SP, 2022.

Vários escoamentos de interesse prático são de fluidos viscoelásticos. Devido à aplicabilidade industrial desse tipo de escoamento, é desejável saber como esse escoamento se propaga caso apareçam perturbações no sistema. Supondo que perturbações sejam introduzidas no sistema, dependendo das características do escoamento e do fluido, este pode sofrer uma transição para um estado turbulento, que podem gerar danos às estruturas e até o rompimento de tubulações. A hidrodinâmica dos fluidos viscoelásticos é fortemente afetada pela interação entre as forças inerciais, viscosas e elásticas. A técnica da Teoria da Estabilidade Linear (LST) investiga a propagação das perturbações no escoamento. Esta técnica consiste em resolver um problema de autovalor/autovetor, onde o autovalor mais instável carrega informações quanto a estabilidade do escoamento estudado (a taxa de amplificação das ondas de Tollmien-Schlichting). Este problema de autovalor é resolvido através da função EIG no software MATLAB. Ao resolver este problema de autovalor de forma direta, todo o autoespectro é obtido, entre eles o autovalor que carrega a informação de estabilidade do escoamento. As autofunções associadas a este autovalor também são obtidas, possibilitando a análise da energia das perturbações. Existem muitas formas de se analisar a estabilidade de um escoamento, ao qual as mais comuns são através da taxa de amplificação das perturbações e através da análise da energia dessas perturbações. Na presente pesquisa, a transição laminar-turbulenta é estudada investigando a propagação das ondas de Tollmien-Schlichting. Adotou-se um escoamento de fluido viscoelástico incompressível em um canal tridimensional. As equações constitutivas adotadas foram os modelos Upper-Convected Maxwell (UCM), Oldroyd-B, Giesekus e Linear Phan-Thien-Tanner (LPTT). A análise de estabilidade é realizada verificando a taxa de amplificação das perturbações e construindo um diagrama de estabilidade. Este diagrama é chamado de curva de estabilidade neutra. Para o fluido Oldroyd-B foi verificado que o aumento da contribuição do solvente na mistura estabiliza o escoamento. Para o modelo UCM foi verificado que o aumento da elasticidade desestabiliza o escoamento, tanto para baixas quanto para frequências mais elevadas. Para o modelo Giesekus foi verificado que maiores quantidade de polímero na mistura estabiliza o escoamento para baixos valores do parâmetro desse modelo, e que conforme o valor deste parâmetro aumenta, o escoamento se torna mais instável.

Palavras-chave: Teoria de Estabilidade Linear, Modelo UCM, Modelo Oldroyd-B, Modelo Giesekus, Modelo LPTT.

ABSTRACT

FURLAN, L. J. S. **Linear Stability Theory Applied to Three-Dimensional Viscoelastic Fluid Flows**. 2022. 86 p. Tese (Doutorado em Ciências – Ciências de Computação e Matemática Computacional) – Instituto de Ciências Matemáticas e de Computação, Universidade de São Paulo, São Carlos – SP, 2022.

Several flows of practical interest are viscoelastic fluids. Due to the industrial applicability of this type of flow, it is desirable to know how this flow propagates if disturbances appear in the system. Assuming that disturbances are introduced into the system, depending on the characteristics of the flow and the fluid, it may transition to a turbulent state, which can damage structures and even pipelines to rupture. The interaction between inertial, viscous and elastic forces strongly affects the hydrodynamics of viscoelastic fluids. The Linear Stability Theory (LST) technique investigates the propagation of disturbances in the flow. This technique solves an eigenvalue/ eigenvector problem, where the most unstable eigenvalue carries information regarding the stability of the flow studied (the amplification rate of the Tollmien-Schlichting waves). This eigenvalue problem is solved using the EIG function in MATLAB software. By directly solving this eigenvalue problem, the entire eigen spectrum is obtained, among them the eigenvalue that carries the stability information of the flow. The eigenfunctions associated with this eigenvalue are also obtained, allowing the analysis of the energy of the disturbances. There are many ways to analyze the stability of a flow. The most common is through the amplification rate of disturbances and the analysis of the energy of these disturbances. In the present research, the laminar-turbulent transition is studied by investigating the propagation of Tollmien-Schlichting waves. It adopted an incompressible viscoelastic fluid flow in a three-dimensional channel. The constitutive equations adopted were the UCM (Upper-Convected Maxwell), the Oldroyd-B, the Giesekus, and the linear Phan-Thien-Tanner (LPTT) models. The stability analysis is performed by analyzing the amplification rate of the disturbances and building a stability diagram. This diagram is called the neutral stability curves diagram. In the Oldroyd-B model increasing the solvent contribution in the mixture stabilizes the flow. For the UCM model, the increase in elasticity destabilizes the flow both for lower and higher frequencies. For the Giesekus model, the higher amount of polymer in the mixture stabilizes the flow for lower values of this model's parameter and as the value of this parameter increases, the flow becomes more unstable.

Keywords: Linear Stability Theory, UCM Model, Oldroyd-B Model, Giesekus Model, LPTT Model.

LIST OF FIGURES

LIST OF TABLES

LIST OF ABBREVIATIONS AND ACRONYMS

DNS	Direct Numerical Simulation
LPOG	"LP" is a reference to the linear Phan-Thien-Tanner viscoelastic model, "O" corresponds to the Oldroyd-B (UCM) model, and "G" refers to the Giesekus model
LPTT	Linear Phan-Thien-Tanner
LST	Linear Stability Theory
UCM	Upper-Convected Maxwell

LIST OF SYMBOLS

ρ — density

$\mathbf{u}$ — velocity vector

t — time variable

σ — total stress tensor

p — pressure

$\mathbf{I}$ — matrix identity

τ — symmetric stress tensor

x — longitudinal coordinate

y — latitudinal coordinate

z — transverse coordinate

η_s — newtonian solvent viscosity

$\mathbf{D}$ — strain rate tensor

$\mathbf{T}$ — extra-stress tensor

η_p — polymeric viscosity coefficient

λ — fluid relaxation time

α_G — parameter of the Giesekus model

ξ — positive parameter of the PTT model

ε — parameter of the PTT model

Re — Reynolds number

Wi — Weissenberg number

β_{nn} — controls the Newtonian solvent contribution

i — imaginary unit

ω — disturbances frequency

λ_x — wavelength in streamwise direction

λ_z — wavelength in spanwise direction

c — wave speed

α — wavenumber in x direction

β — wavenumber in z direction

ϕ — wave propagation angle

CONTENTS

CHAPTER

1

INTRODUCTION

In many industrial applications, the products are directly related to fluid dynamics. Among the many problems in this area are the treatments of non-Newtonian fluid flows. Increasingly, polymers are replacing other materials, so the polymer product should have a satisfactory mechanical performance during its designed lifetime for a given application. In addition to polymer processing, there are other industrial applications involving viscoelastic fluid flows, such as plastic injection, extrusion processes, and oil extraction, producing many problems to be investigated.

In this sense, with the development of computer technology, there is a great interest in working with the numerical simulations of these industrial applications, developing efficient numerical methods to simulate viscoelastic fluid flows, due to this requiring a low cost of financial resources in comparison to experiments in laboratories. It is possible to obtain excellent results that faithfully represent these fluids' behaviour in various flows. However, this challenge is not simple. The constitutive equations that model viscoelastic fluids are complex and difficult to treat in computational domains.

These materials exhibit both viscous and elastic properties at the same time. They present complex molecules and high molar mass (long and structured molecules). The classical Navier-Stokes equations are unable to describe the flow dynamics of this type of material. An additional constitutive equation is required for the stress field, making the stress components additional unknowns. The usual procedure in choosing constitutive equations is to search for an adequate equation to describe the process to be studied and the set of parameters that maximizes the chosen equation to the type and conditions of the process under study.

In the literature one can find many works dealing with constitutive models of viscoelastic fluids, such as the differentials of MAXWELL ((BERIS; ARMOSTRONG; BROWN, 1987), (MOMPEAN; DEVILLE, 1997)), OLDROYD-B ((BRASSEUR *et al.*, 1994), (MOMPEAN; DEVILLE, 1997), (PHILLIPS; WILLIAMS, 2002), (PINHO; ALVES; OLIVEIRA, 2003)),

White-Metzner (WHITE; METZNER, 1963), Giesekus ((GIESEKUS, 1962), (GIESEKUS, 1982), (GIESEKUS, 1985)), Leonov (LEONOV, 1976), FENE-type models ((BIRD; DOTSON; JOHNSON, 1980), (BIRD; DEAGUIAR, 1983), (CHRISTIANSEN; BIRD, 1977), (STEVENSON; BIRD, 1971), (WARNER, 1972), (OLIVEIRA,)), PTT ((PHAN-THIEN; TANNER, 1977), (PINHO; ALVES; OLIVEIRA, 2003)) and derivatives, Pom Pom (LARSON, 1988) and derivatives; and the integral models: Maxwell (KAYE, 1962) and K-BKZ ((LUO; TANNER, 1986), (LUO; TANNER, 1988)).

Maxwell's model was one of the first attempts to describe the effect of the viscoelasticity of a given fluid. This model incorporates the idea of a fluid that exhibits characteristics of a Hookean elastic solid and Newtonian viscous fluid. The Oldroyd-B model derives from the kinetic theory for concentrated and molten polymer solutions (BIRD; ARMSTRONG; HASSAGER, 1987). The polymer chain is represented by a set of two spheres linked by a spring. In this configuration, the spheres represent the system's centre of mass. They are related to the hydrodynamic interaction between the solvent and the macromolecules of the polymeric solution (the viscous drag force of the solvent on the molecules). The springs represent the elasticity effect of the macromolecules or the restorative effect of the polymer. This ball/spring configuration called "*dumbbell*" is simplified by assuming a linear spring or Hooke spring behaviour. The Oldroyd-B model can well represent certain fluids with ideal elasticity, also known as "Boger" fluids.

The rheological model developed by Giesekus (1982) is also based on molecular considerations with ball/spring systems where the spring follows Hooke's law. Differently from the Oldroyd-B model, in the Giesekus model, a non-isotropy effect was introduced in the definition of the drag force on the spheres. This model results in an equation with the form analogous to the UCM and Oldroyd-B models but containing non-linear terms given by the products between the stress tensor. Another model widely used in numerical simulations of viscoelastic fluids is the Phan-Thien-Tanner model (PHAN-THIEN; TANNER, 1977), known as PTT. This model is derived from the *network theory of concentrated solutions and melts* and considers the network's elastic energy.

Hydrodynamic stability theory is concerned with the response of a laminar flow to a disturbance of small or moderate amplitude. Every fluid flow is subject to small disturbances due to various factors, such as structural vibration, surface roughness, noise, and external turbulence. If these disturbances are not smoothed, the laminar flow can suffer a transition to another, more complex state, but not necessarily a turbulent flow state (SOUZA; MENDONÇA; MEDEIROS, 2005). The process by which a laminar flow becomes turbulent is known as the laminar-turbulent transition (SCHMID; HENNINGSON, 2001). This is a highly complex process that, at present, is still not fully understood. However, after decades of intense research, specific characteristics have gradually become apparent, primarily for Newtonian fluid flows.

For any fluid flow, the transition to turbulence can be generalized as the result of the

amplification of disturbances that can arise in the fluid flows. If a field of an unsteady (usually laminar) flow that is at equilibrium is disturbed slightly at a certain point in space and time, the result will be an even more substantial variation (amplification of the disturbance) than an equilibrium farther away in space (spatial instability) or time (temporal instability). This variation can be measured in terms of the energy or the amplification rate of the disturbances (MARXEN, 2005).

In general, the arising of instabilities in Newtonian flows is a direct consequence of the presence of the convective term in the momentum equation, which has the function of amplifying with increasing Reynolds number (as the value of Re increases, the influence of the viscous terms, which are dissipative, decreases. In fact, for high values of Re, the viscosity becomes destabilizing due to the viscous friction effect within the boundary layer). However, in viscoelastic flows, nonlinearities enter through convection in the momentum equation and through convection in the tensor equation from the constitutive equation.

Draad, Kuiken and Nieuwstadt (1998) reported transition delay for viscoelastic fluid flows; that is, the onset was postponed to a higher Reynolds number than Newtonian fluid flows. In another study, Ram and Tamir (1964) observed that turbulence sets in at a Reynolds number smaller than in the Newtonian case, a phenomenon called “early turbulence”. It has recently been demonstrated that at a large Weissenberg number, the anisotropic elastic stresses destabilize flows with curved streamlines even in the absence of inertia, resulting in so-called “purely elastic linear instabilities” (SAMANTA *et al.*, 2013). It is clear that the instability for viscoelastic fluid flows is neither inertial since it exists at a zero Reynolds number (CASTILLO; WILSON, 2017).

In recent years, several purely elastic instabilities have been reported corresponding to experimental or theoretical work using linear stability analysis (LIM; SCHOWALTER, 1987; LEE; FINLAYSON, 1986; LARSON; SHAQFEH; MULLER, 1990; SHAQFEH; MULLER; LARSON, 1992; LARSON, 1992). In most works on this type of analysis in viscoelastic flows, the UCM and Oldroyd-B constitutive models have been employed, and the choice of model for the constitutive equation directly affects the stability analysis results. For example, the Oldroyd-B model shows more stabilization than the UCM model in a parallel flow when the solvent viscosity is taken into account (SURESHKUMAR; BERIS, 1995). Therefore, there are several works in the literature that perform stability analysis for other types of viscoelastic models where parallel flows are generally used as *benchmark* tests (see (AVGOUSTI; BERIS, 1993; SURESHKUMAR; BERIS, 1995; BLONCE, 1997; MAK, 2009; ZHANG *et al.*, 2013; GERVAZONI, 2016; SOUZA; BRANDI; MENDONçA, 2016; SILVA, 2018; FURLAN, 2018; BRANDI; MENDONçA; SOUZA, 2019)).

Even today, studies in parallel flows have not been widely developed, and some questions remain unanswered. Zhang et al. (ZHANG *et al.*, 2013) investigated modal and non-modal stability for channel flow for the FENE-P and Oldroyd-B fluid models. The main conclusion was that the effect of the polymer could be characterized by the ratio between the relaxation time

and the time scale during which the instability evolves; this applies to the exponential growth of two-dimensional Tollmien-Schlichting waves and the non-modal amplification of elongated streaks in the flow direction and oblique waves in the subcritical regime.

In this work, the interest is in numerical results for stability analysis of three-dimensional flows of viscoelastic fluids, considering different flow characteristics, such as the amount of polymer viscosity in the mixture (fully polymeric fluid flow and with solvent viscosity contribution) and different values of the Weissenberg number. To that end, the Linear Stability Theory (MENDONÇA; MEDEIROS, 2002) was used to analyze the stability of viscoelastic fluid flows, particularly in the problem of three-dimensional, incompressible parallel flow for the constitutive models UCM, Oldroyd-B, Giesekus and LPTT. For this purpose, a different way of solving the stability problem is presented, using the system of linearized equations, rewriting them into an eigenvalue problem and solving this problem through the matrix method.

1.1 Outline

This thesis is organized as follows:

Chapter 2 presents the governing equations for three-dimensional, incompressible, isothermal flow for a non-Newtonian fluid. The equation considered in viscoelastic flow is the constitutive equation called here as LPOG, and consists of an equation containing four viscoelastic models where the LPOG equation becomes the desired model from the assignment of the "zero" value for the dimensionless parameters of the unwanted models.

Chapter 3 presents a theoretical study to verify the validity of Squire's theorem (SQUIRE, 1933) for viscoelastic fluid flows.

Chapter 4 presents the laminar flows used in this work to obtain the results regarding the stability of the models' viscoelastic flows and the solution method for the eigenvalue problem associated with the stability analysis problem.

Chapter 5 presents the results obtained to analyze the stability of the flows for the viscoelastic models considered in this work, such as amplification rates and the neutral stability curves, varying the dimensionless parameters of each model, as well as the amount of viscosity of the solvent in the mixture and also the Weissenberg number.

The main conclusions of the work are presented in Chapter 6.

Appendix A presents the algebraic manipulations needed to rewrite the system of equations into an eigenvalue/eigenvector problem. Appendix **??** presents the algorithm used to calculate the derivatives using Chebyshev polynomials.

CHAPTER

2

MATHEMATICAL FORMULATION

This chapter presents the governing equations for incompressible, isothermal, three-dimensional flows for viscoelastic fluids. The equations describing fluctuations for three-dimensional viscoelastic fluid flows are obtained using Linear Stability Theory.

2.1 Governing Equations

Incompressible and isothermal, three-dimensional flows are governed by the equation of conservation of mass (the continuity equation)

$$\nabla \cdot \mathbf{u} = 0, \tag{2.1}$$

and by the equation of conservation of momentum

$$\rho \left(\frac{\partial \mathbf{u}}{\partial t} + \nabla \cdot (\mathbf{u}\mathbf{u}) \right) = \nabla \cdot \sigma, \tag{2.2}$$

where ρ is the specific mass of the fluid (density), $\mathbf{u}$ is the velocity vector, t is time. The variable σ is the total stress tensor, defined by

$$\sigma = \tau - p\mathbf{I}, \tag{2.3}$$

where p is the pressure, $\mathbf{I}$ is the identity tensor and τ is the symmetric extra-stress tensor, defined by the constitutive equation of the fluid considered in the simulation. In the three-dimensional case, $\mathbf{u} = [u \;\; v \;\; w]^T$ represents the velocity components in the directions x, y and z, respectively.

Non-Newtonian fluids are those fluids that do not exhibit linearity between strain rate and shear stress. The dynamic viscosity value is not constant, i.e. it varies with the applied strain rate (TANNER, 1988). In the viscoelastic fluid model, the symmetric extra-stress tensor is defined by the sum of the Newtonian contribution (viscous) and the non-Newtonian contribution (elastic) (RAJAGOPALAN; ARMSTRONG; BROWN, 1990), that is,

$$\tau = 2\eta_s \mathbf{D} + \mathbf{T}, \tag{2.4}$$

where η_s is the viscosity of the Newtonian solvent, $\mathbf{D}$ is the strain rate tensor defined by $\mathbf{D} = \frac{1}{2}(\nabla\mathbf{u} + (\nabla\mathbf{u})^T)$ and $\mathbf{T}$ is the extra-stress tensor (symmetric) that represents the non-Newtonian contribution, with three-dimensional components of the form $\mathbf{T} = \begin{bmatrix} T^{xx} & T^{xy} & T^{xz} \\ T^{xy} & T^{yy} & T^{yz} \\ T^{xz} & T^{yz} & T^{zz} \end{bmatrix}$.

Therefore, by calculating the divergence of the total stress tensor (2.3), the modified momentum equation for a viscoelastic fluid is obtained

$$\rho\left(\frac{\partial\mathbf{u}}{\partial t} + \nabla\cdot(\mathbf{uu})\right) = -\nabla\cdot p\mathbf{I} + \eta_s\nabla^2\cdot\mathbf{u} + \nabla\cdot\mathbf{T}. \tag{2.5}$$

In this work, the LPOG constitutive equation (BERIS; ARMOSTRONG; BROWN, 1987; BRASSEUR *et al.*, 1994; PHAN-THIEN; TANNER, 1977; GIESEKUS, 1982) was considered for the viscoelastic fluid model, which is defined as follows

$$\begin{aligned}\left(1+\frac{\varepsilon\lambda}{\eta_p}ft(\mathbf{T})\right)\mathbf{T} + \lambda\left(\frac{\partial\mathbf{T}}{\partial t} + \nabla\cdot(\mathbf{uT}) - \nabla\mathbf{u}\cdot\mathbf{T} - \mathbf{T}\cdot\nabla\mathbf{u}^T\right) + \xi\lambda\left(\mathbf{D}\cdot\mathbf{T} + \mathbf{T}\cdot\mathbf{D}^T\right) + \\ + \frac{\alpha_G\lambda}{\eta_p}(\mathbf{T}\cdot\mathbf{T}) = 2\eta_p\mathbf{D},\end{aligned} \tag{2.6}$$

where η_p is the polymeric viscosity coefficient, λ is the fluid relaxation time, the constant α_G represents the mobility parameter that regulates the shear thinning behavior of the fluid ($0 \leq \alpha_G \leq 0.5$), and it is a Giesekus model parameter. The term's origin involving α_G can be associated with the anisotropic hydrodynamic drag on the constituent polymer molecules (BIRD; ARMSTRONG; HASSAGER, 1987). ξ is a positive parameter of the PTT model and relates to the differences in normal stresses. The ε parameter is related to the elongational behaviour of the fluid, excluding the possibility of an infinite elongational viscosity in a simple stretching flow, as would occur for a Maxwell model (UCM or Oldroyd-B) when $\varepsilon = 0$ (PINHO; OLIVEIRA, 2000), and is a parameter of the PTT model. This parameter is related to its extensional properties: when a fluid filament is stretched axially, the higher the stretching opposition is, the smaller ε. The term $ft(\mathbf{T})$ denotes the trace function of the tensor $\mathbf{T}$, and $\mathbf{T}\cdot\mathbf{T}$ denotes the tensor product.

Therefore, in the constitutive equation referred to here as LPOG (2.6), we have "four" possible viscoelastic models. These are:

- UCM e Oldroyd-B $\rightarrow \alpha_G = \varepsilon = \xi = 0$;
- Giesekus $\rightarrow \varepsilon = \xi = 0$;
- LPTT $\rightarrow \alpha_G = 0$.

2.2 Dimensionless Equations

The equations (2.1) - (2.5) model incompressible, isothermal, viscoelastic flows, and have been presented in dimensional form. However, it is convenient to solve the equations in

their dimensionless form. It facilitates the visualization of physical effects, the formulation of the model independent of the system of units, limitation of values for variables and parameters. Most importantly, it provides conditions for geometrically similar situations to be obtained. Requires the following variable changes:

$$\mathbf{x}^* = \frac{\mathbf{x}}{L}, \ \mathbf{u}^* = \frac{\mathbf{u}}{U}, \ t^* = \frac{U}{L}t,$$

$$p^* = \frac{p}{\rho U^2}, \ \tau^* = \frac{\tau}{\rho U^2}, \ \mathbf{T}^* = \frac{\mathbf{T}}{\rho U^2},$$

where L is the half-width channel, and U is a velocity scale. Substituting these variables into the equations (2.1),(2.5), (2.6), the dimensionless governing equations are obtained (to simplify notation, the "$*$" sign has been omitted from the equations)

$$\nabla \cdot \mathbf{u} = 0, \tag{2.7}$$

$$\frac{\partial \mathbf{u}}{\partial t} + \nabla \cdot (\mathbf{uu}) = -\nabla p\mathbf{I} + \frac{\beta_{nn}}{Re}\nabla^2\mathbf{u} + \nabla \cdot \mathbf{T}, \tag{2.8}$$

$$\begin{aligned}\left(1 + \frac{\varepsilon WiRe}{(1-\beta_{nn})} ft(\mathbf{T})\right)\mathbf{T} + Wi\left(\frac{\partial \mathbf{T}}{\partial t} + \nabla \cdot (\mathbf{uT}) - \nabla\mathbf{u}\cdot\mathbf{T} - \mathbf{T}\cdot\nabla\mathbf{u}^T\right) + \\ + \xi Wi\left(\mathbf{D}\cdot\mathbf{T} + \mathbf{T}\cdot\mathbf{D}^T\right) + \frac{\alpha_G ReWi}{(1-\beta_{nn})}(\mathbf{T}\cdot\mathbf{T}) = 2\frac{(1-\beta_{nn})}{Re}\mathbf{D}.\end{aligned} \tag{2.9}$$

Considering the changes in the variables system, dimensionless constants appear in the equations. These constants are known in the literature as the Reynolds number, defined by $Re = \dfrac{\rho UL}{\eta_0}$ (it is the ratio between the inertial forces and the viscous forces of the flow), the Weissenberg number $Wi = \dfrac{\lambda U}{L}$ (for a viscoelastic fluid, it is the ratio between the elastic forces and the viscous forces) and the constant $\beta_{nn} = \dfrac{\eta_s}{\eta_0}$, where $\beta_{nn} \in [0,1)$ (it is the constant that controls the Newtonian solvent contribution. The closer to 0 are the value of β_{nn}, the more non-Newtonian the fluid flow, to the point that $\beta_{nn} = 0$ is a purely polymeric fluid flow). The constant η_0 represents the total viscosity of the flow, and is defined as the sum of the solvent viscosity and the polymer viscosity $\eta_0 = \eta_s + \eta_p$.

Rewriting the three-dimensional equations is obtained.

$$\frac{\partial u}{\partial x} + \frac{\partial v}{\partial y} + \frac{\partial w}{\partial z} = 0, \tag{2.10}$$

$$\frac{\partial u}{\partial t} + \frac{\partial uu}{\partial x} + \frac{\partial uv}{\partial y} + \frac{\partial uw}{\partial z} = -\frac{\partial p}{\partial x} + \frac{\beta_{nn}}{Re}\left[\frac{\partial^2 u}{\partial x^2} + \frac{\partial^2 u}{\partial y^2} + \frac{\partial^2 u}{\partial z^2}\right] + \frac{\partial T_{xx}}{\partial x} + \frac{\partial T_{xy}}{\partial y} + \frac{\partial T_{xz}}{\partial z}, \tag{2.11}$$

$$\frac{\partial v}{\partial t}+\frac{\partial vu}{\partial x}+\frac{\partial vv}{\partial y}+\frac{\partial vw}{\partial z}=-\frac{\partial p}{\partial y}+\frac{\beta_{nn}}{Re}\left[\frac{\partial^2 v}{\partial x^2}+\frac{\partial^2 v}{\partial y^2}+\frac{\partial^2 v}{\partial z^2}\right]+\frac{\partial T_{xy}}{\partial x}+\frac{\partial T_{yy}}{\partial y}+\frac{\partial T_{yz}}{\partial z}, \quad (2.12)$$

$$\frac{\partial w}{\partial t}+\frac{\partial wu}{\partial x}+\frac{\partial wv}{\partial y}+\frac{\partial ww}{\partial z}=-\frac{\partial p}{\partial z}+\frac{\beta_{nn}}{Re}\left[\frac{\partial^2 w}{\partial x^2}+\frac{\partial^2 w}{\partial y^2}+\frac{\partial^2 w}{\partial z^2}\right]+\frac{\partial T_{xz}}{\partial x}+\frac{\partial T_{yz}}{\partial y}+\frac{\partial T_{zz}}{\partial z}, \quad (2.13)$$

$$\begin{aligned}T_{xx}+\frac{\varepsilon ReWi}{(1-\beta_{nn})}\Big(T_{xx}+T_{yy}+T_{zz}\Big)T_{xx}+Wi\Bigg(&\frac{\partial T_{xx}}{\partial t}+\frac{\partial(uT_{xx})}{\partial x}+\frac{\partial(vT_{xx})}{\partial y}+\frac{\partial(wT_{xx})}{\partial z}+\\&-2T_{xx}\frac{\partial u}{\partial x}-2T_{xy}\frac{\partial u}{\partial y}-2T_{xz}\frac{\partial u}{\partial z}+\xi\Bigg[2T_{xx}\frac{\partial u}{\partial x}+T_{xy}\left(\frac{\partial u}{\partial y}+\frac{\partial v}{\partial x}\right)+\\&+T_{xz}\left(\frac{\partial u}{\partial z}+\frac{\partial w}{\partial x}\right)\Bigg]\Bigg)+\frac{\alpha_G ReWi}{(1-\beta_{nn})}\Big(T_{xx}^2+T_{xy}^2+T_{xz}^2\Big)=\frac{2(1-\beta_{nn})}{Re}\frac{\partial u}{\partial x},\end{aligned} \quad (2.14)$$

$$\begin{aligned}T_{xy}+\frac{\varepsilon ReWi}{(1-\beta_{nn})}\Big(T_{xx}+T_{yy}+T_{zz}\Big)T_{xy}+Wi\Bigg(&\frac{\partial T_{xy}}{\partial t}+\frac{\partial(uT_{xy})}{\partial x}+\frac{\partial(vT_{xy})}{\partial y}+\frac{\partial(wT_{xy})}{\partial z}+\\&-T_{xx}\frac{\partial v}{\partial x}-T_{xy}\frac{\partial v}{\partial y}-T_{xz}\frac{\partial v}{\partial z}-T_{xy}\frac{\partial u}{\partial x}-T_{yy}\frac{\partial u}{\partial y}-T_{yz}\frac{\partial u}{\partial z}+\xi\Bigg[T_{xy}\frac{\partial u}{\partial x}+\frac{1}{2}T_{yy}\left(\frac{\partial u}{\partial y}+\right.\\&\left.+\frac{\partial v}{\partial x}\right)+\frac{1}{2}T_{yz}\left(\frac{\partial u}{\partial z}+\frac{\partial w}{\partial x}\right)+\frac{1}{2}T_{xx}\left(\frac{\partial u}{\partial y}+\frac{\partial v}{\partial x}\right)+T_{xy}\frac{\partial v}{\partial y}+\frac{1}{2}T_{xz}\left(\frac{\partial w}{\partial y}+\right.\\&\left.+\frac{\partial v}{\partial z}\right)\Bigg]\Bigg)+\frac{\alpha_G ReWi}{(1-\beta_{nn})}\Big(T_{xx}T_{xy}+T_{xy}T_{yy}+T_{xz}T_{yz}\Big)=\frac{(1-\beta_{nn})}{Re}\left(\frac{\partial u}{\partial y}+\frac{\partial v}{\partial x}\right),\end{aligned} \quad (2.15)$$

$$\begin{aligned}T_{xz}+\frac{\varepsilon ReWi}{(1-\beta_{nn})}\Big(T_{xx}+T_{yy}+T_{zz}\Big)T_{xz}+Wi\Bigg(&\frac{\partial T_{xz}}{\partial t}+\frac{\partial(uT_{xz})}{\partial x}+\frac{\partial(vT_{xz})}{\partial y}+\frac{\partial(wT_{xz})}{\partial z}+\\&-T_{xx}\frac{\partial w}{\partial x}-T_{xy}\frac{\partial w}{\partial y}-T_{xz}\frac{\partial w}{\partial z}-T_{xz}\frac{\partial u}{\partial x}-T_{yz}\frac{\partial u}{\partial y}-T_{zz}\frac{\partial u}{\partial z}+\xi\Bigg[T_{xz}\frac{\partial u}{\partial x}+\frac{1}{2}T_{yz}\left(\frac{\partial u}{\partial y}+\right.\\&\left.+\frac{\partial v}{\partial x}\right)+\frac{1}{2}T_{zz}\left(\frac{\partial u}{\partial z}+\frac{\partial w}{\partial x}\right)+\frac{1}{2}T_{xx}\left(\frac{\partial w}{\partial x}+\frac{\partial u}{\partial z}\right)+\frac{1}{2}T_{xy}\left(\frac{\partial w}{\partial y}+\frac{\partial v}{\partial z}\right)+\\&+T_{xz}\frac{\partial w}{\partial z}\Bigg]\Bigg)+\frac{\alpha_G ReWi}{(1-\beta_{nn})}\Big(T_{xx}T_{xz}+T_{xy}T_{yz}+T_{xz}T_{zz}\Big)=\frac{(1-\beta_{nn})}{Re}\left(\frac{\partial u}{\partial z}+\frac{\partial w}{\partial x}\right),\end{aligned} \quad (2.16)$$

$$\begin{aligned}T_{yy}+\frac{\varepsilon ReWi}{(1-\beta_{nn})}\Big(T_{xx}+T_{yy}+T_{zz}\Big)T_{yy}+Wi\Bigg(&\frac{\partial T_{yy}}{\partial t}+\frac{\partial(uT_{yy})}{\partial x}+\frac{\partial(vT_{yy})}{\partial y}+\frac{\partial(wT_{yy})}{\partial z}+\\&-2T_{xy}\frac{\partial v}{\partial x}-2T_{yy}\frac{\partial v}{\partial y}-2T_{yz}\frac{\partial v}{\partial z}+\xi\Bigg[T_{xy}\left(\frac{\partial v}{\partial x}+\frac{\partial u}{\partial y}\right)+2T_{yy}\frac{\partial v}{\partial y}+\\&+T_{yz}\left(\frac{\partial v}{\partial z}+\frac{\partial w}{\partial y}\right)\Bigg]\Bigg)+\frac{\alpha_G ReWi}{(1-\beta_{nn})}\Big(T_{xy}^2+T_{yy}^2+T_{yz}^2\Big)=\frac{2(1-\beta_{nn})}{Re}\frac{\partial v}{\partial y},\end{aligned} \quad (2.17)$$

$$T_{yz}+\frac{\varepsilon ReWi}{(1-\beta_{nn})}\Big(T_{xx}+T_{yy}+T_{zz}\Big)T_{yz}+Wi\Bigg(\frac{\partial T_{yz}}{\partial t}+\frac{\partial(uT_{yz})}{\partial x}+\frac{\partial(vT_{yz})}{\partial y}+\frac{\partial(wT_{yz})}{\partial z}+$$
$$-T_{xy}\frac{\partial w}{\partial x}-T_{yy}\frac{\partial w}{\partial y}-T_{yz}\frac{\partial w}{\partial z}-T_{xz}\frac{\partial v}{\partial x}-T_{yz}\frac{\partial v}{\partial y}-T_{zz}\frac{\partial v}{\partial z}+\xi\Bigg[\frac{1}{2}T_{xz}\left(\frac{\partial v}{\partial x}+\frac{\partial u}{\partial y}\right)+$$
$$+T_{yz}\frac{\partial v}{\partial y}+\frac{1}{2}T_{zz}\left(\frac{\partial v}{\partial z}+\frac{\partial w}{\partial y}\right)+\frac{1}{2}T_{xy}\left(\frac{\partial w}{\partial x}+\frac{\partial u}{\partial z}\right)+\frac{1}{2}T_{yy}\left(\frac{\partial w}{\partial y}+\frac{\partial v}{\partial z}\right)+$$
$$+T_{yz}\frac{\partial w}{\partial z}\Bigg]\Bigg)+\frac{\alpha_G ReWi}{(1-\beta_{nn})}\Big(T_{xy}T_{xz}+T_{yy}T_{yz}+T_{yz}T_{zz}\Big)=\frac{(1-\beta_{nn})}{Re}\left(\frac{\partial v}{\partial z}+\frac{\partial w}{\partial y}\right), \tag{2.18}$$

$$T_{zz}+\frac{\varepsilon ReWi}{(1-\beta_{nn})}\Big(T_{xx}+T_{yy}+T_{zz}\Big)T_{zz}+Wi\Bigg(\frac{\partial T_{zz}}{\partial t}+\frac{\partial(uT_{zz})}{\partial x}+\frac{\partial(vT_{zz})}{\partial y}+\frac{\partial(wT_{zz})}{\partial z}+$$
$$-2T_{xz}\frac{\partial w}{\partial x}-2T_{yz}\frac{\partial w}{\partial y}-2T_{zz}\frac{\partial w}{\partial z}+\xi\Bigg[T_{xz}\left(\frac{\partial w}{\partial x}+\frac{\partial u}{\partial z}\right)+T_{yz}\left(\frac{\partial w}{\partial y}+\frac{\partial v}{\partial z}\right)+$$
$$+2T_{zz}\frac{\partial w}{\partial z}\Bigg]\Bigg)+\frac{\alpha_G ReWi}{(1-\beta_{nn})}\Big(T_{xz}^2+T_{yz}^2+T_{zz}^2\Big)=\frac{2(1-\beta_{nn})}{Re}\frac{\partial w}{\partial z}. \tag{2.19}$$

The set equations (2.10) - (2.19) model the three-dimensional flow of viscoelastic, incompressible, isothermal fluids, for the UCM ($\beta_{nn}=\alpha_G=\varepsilon=\xi=0$), Oldroyd-B ($\alpha_G=\varepsilon=\xi=0$), Giesekus ($\varepsilon=\xi=0$), and LPTT ($\alpha_G=0$) models.

2.3 Linear Stability Theory

Through the Linear Stability Theory, the stability analysis of viscoelastic fluid flows is carried out in this work, considering the LPOG constitutive equation.

The LST technique analyzes the behaviour of a flow if disturbances of infinitesimal amplitude are introduced. Assuming the instantaneous flow can decompose into a laminar and a disturbing part. Therefore, the dependent variables can be decomposed as follows:

$$\begin{aligned} u(x,y,z,t) &= U(y)+\tilde{u}(x,y,z,t),\\ v(x,y,z,t) &= \tilde{v}(x,y,z,t),\\ w(x,y,z,t) &= \tilde{w}(x,y,z,t),\\ p(x,y,z,t) &= P(x,y)+\tilde{p}(x,y,z,t). \end{aligned} \tag{2.20}$$

The non-Newtonian tensors are decomposed in the form

$$T(x,y,z,t)=Tb(y)+\tilde{T}(x,y,z,t), \tag{2.21}$$

where the components of the laminar flow are $U(y), P(x,y)$ and $Tb(y)$. The components of the disturbed flow (perturbations) are represented in the form $\tilde{u}$. The non-Newtonian tensor components Tb_{xz}, Tb_{yz} and Tb_{zz} are zero for the laminar flow.

Laminar flow (baseflow) is assumed invariant in the x-direction. By the continuity equation, the normal-wall component of the mean velocity is zero (the laminar flow is parallel). The laminar flow is assumed to be unvarying over time. Substituting this decomposition into the equations (2.10) - (2.19) and subtracting from the resulting equations the equations satisfied by the laminar flow, it is obtained the linear equations with coefficients not depending on t, x, and z. Therefore, a solution in terms of normal modes may be sought for the disturbances $\tilde{u}, \tilde{v}, \tilde{w}, \tilde{p}$ and $\tilde{T}$ as follows:

$$\begin{aligned}
\tilde{u}(x,y,z,t) &= \frac{1}{2}\left[\overline{u}(y)e^{i(\alpha x+\beta z-\omega t)} + cc.\right], \\
\tilde{v}(x,y,z,t) &= \frac{1}{2}\left[\overline{v}(y)e^{i(\alpha x+\beta z-\omega t)} + cc.\right], \\
\tilde{w}(x,y,z,t) &= \frac{1}{2}\left[\overline{w}(y)e^{i(\alpha x+\beta z-\omega t)} + cc.\right], \\
\tilde{p}(x,y,z,t) &= \frac{1}{2}\left[\overline{p}(y)e^{i(\alpha x+\beta z-\omega t)} + cc.\right], \\
\tilde{T}(x,y,z,t) &= \frac{1}{2}\left[\overline{T}(y)e^{i(\alpha x+\beta z-\omega t)} + cc.\right],
\end{aligned} \tag{2.22}$$

with $i = \sqrt{-1}$. These equations indicate that the disturbances propagate as waves, with frequency ω, wavelength in streamwise direction $\lambda_x = \frac{2\pi}{\alpha}$, wavelength in spanwise direction $\lambda_z = \frac{2\pi}{\beta}$, wave speed $c = \frac{\omega}{\alpha}$, with α is the wavenumber in x direction and β is the wavenumber in z direction, and the respective amplitudes $\overline{u}, \overline{v}, \overline{w}, \overline{p}$ and $\overline{T}$. A three-dimensional wave propagates at an angle ϕ to the direction of laminar flow, such that:

$$\tan\phi = \frac{\beta}{\alpha}. \tag{2.23}$$

Rewriting the system of equations for the flow disturbances using the solutions obtained by normal modes, the equations for the three-dimensional disturbances are obtained

$$i\alpha u + i\beta w + \frac{dv}{dy} = 0, \tag{2.24}$$

$$-i\omega u + iU\alpha u + v\frac{dU}{dy} = -i\alpha p + \frac{\beta_{nn}}{Re}\left(-(\alpha^2+\beta^2)u + \frac{d^2u}{dy^2}\right) + i\alpha T_{xx} + \frac{dT_{xy}}{dy} + i\beta T_{xz}, \tag{2.25}$$

$$-i\omega v + iU\alpha v = -\frac{dp}{dy} + \frac{\beta_{nn}}{Re}\left(-(\alpha^2+\beta^2)v + \frac{d^2v}{dy^2}\right) + i\alpha T_{xy} + \frac{dT_{yy}}{dy} + i\beta T_{yz}, \tag{2.26}$$

$$-i\omega w + iU\alpha w = -i\beta p + \frac{\beta_{nn}}{Re}\left(-(\alpha^2+\beta^2)w + \frac{d^2w}{dy^2}\right) + i\alpha T_{xz} + \frac{dT_{yz}}{dy} + i\beta T_{zz}, \tag{2.27}$$

$$\begin{aligned} T_{xx} + \frac{\varepsilon ReWi}{(1-\beta_{nn})}\Big(T_{xx}+T_{yy}+T_{zz}\Big)Tb_{xx} + \frac{\varepsilon ReWi}{(1-\beta_{nn})}\Big(Tb_{xx}+Tb_{yy}\Big)T_{xx} + Wi\Bigg(-i\omega T_{xx} + \\ +i\alpha U T_{xx} - 2i\alpha Tb_{xx}u + \frac{dTb_{xx}}{dy}v - 2\frac{dU}{dy}T_{xy} - 2Tb_{xy}\frac{du}{dy} + \xi\Bigg[2i\alpha Tb_{xx}u + \frac{dU}{dy}T_{xy} + \\ +Tb_{xy}\left(\frac{du}{dy}+i\alpha v\right)\Bigg]\Bigg) + \frac{2\alpha_G WiRe}{(1-\beta_{nn})}\Big(Tb_{xx}T_{xx}+Tb_{xy}T_{xy}\Big) = \frac{2i\alpha(1-\beta_{nn})}{Re}u, \end{aligned} \tag{2.28}$$

$$\begin{aligned} T_{xy} + \frac{\varepsilon ReWi}{(1-\beta_{nn})}\Big(T_{xx}+T_{yy}+T_{zz}\Big)Tb_{xy} + \frac{\varepsilon ReWi}{(1-\beta_{nn})}\Big(Tb_{xx}+Tb_{yy}\Big)T_{xy} + Wi\Bigg(-i\omega T_{xy} + \\ +i\alpha U T_{xy} - i\alpha Tb_{xx}v + i\beta Tb_{xy}w + \frac{dTb_{xy}}{dy}v - \frac{dU}{dy}T_{yy} - Tb_{yy}\frac{du}{dy} + \xi\Bigg[i\alpha Tb_{xy}u + \\ +\frac{1}{2}\frac{dU}{dy}T_{yy} + \frac{1}{2}Tb_{yy}\left(\frac{du}{dy}+i\alpha v\right) + \frac{1}{2}\frac{dU}{dy}T_{xx} + \frac{1}{2}Tb_{xx}\left(\frac{du}{dy}+i\alpha v\right) + Tb_{xy}\frac{dv}{dy}\Bigg]\Bigg) + \\ +\frac{\alpha_G WiRe}{(1-\beta_{nn})}\Big(Tb_{xy}\big(T_{xx}+T_{yy}\big) + T_{xy}\big(Tb_{xx}+Tb_{yy}\big)\Big) = \frac{(1-\beta_{nn})}{Re}\left(\frac{du}{dy}+i\alpha v\right), \end{aligned} \tag{2.29}$$

$$\begin{aligned} T_{xz} + \frac{\varepsilon ReWi}{(1-\beta_{nn})}\Big(Tb_{xx}+Tb_{yy}\Big)T_{xz} + Wi\Bigg(-i\omega T_{xz} + i\alpha U T_{xz} - i\alpha Tb_{xx}w - Tb_{xy}\frac{dw}{dy} + \\ -\frac{dU}{dy}T_{yz} + \xi\left[\frac{1}{2}T_{yz}\frac{dU}{dy} + \frac{1}{2}Tb_{xx}(i\beta u + i\alpha w) + \frac{1}{2}Tb_{xy}\left(i\beta v + \frac{dw}{dy}\right)\right]\Bigg) + \\ +\frac{\alpha_G WiRe}{(1-\beta_{nn})}\Big(Tb_{xx}T_{xz}+Tb_{xy}T_{yz}\Big) = \frac{(1-\beta_{nn})}{Re}\Big(i\beta u + i\alpha w\Big), \end{aligned} \tag{2.30}$$

$$\begin{aligned} T_{yy} + \frac{\varepsilon ReWi}{(1-\beta_{nn})}\Big(T_{xx}+T_{yy}+T_{zz}\Big)Tb_{yy} + \frac{\varepsilon ReWi}{(1-\beta_{nn})}\Big(Tb_{xx}+Tb_{yy}\Big)T_{yy} + Wi\Bigg(-i\omega T_{yy} + \\ +i\alpha U T_{yy} + \frac{dTb_{yy}}{dy}v - 2i\alpha Tb_{xy}v - 2Tb_{yy}\frac{dv}{dy} + \xi\Bigg[\frac{dU}{dy}T_{xy} + Tb_{xy}\left(\frac{du}{dy}+i\alpha v\right) + \\ +2Tb_{yy}\frac{dv}{dy}\Bigg]\Bigg) + \frac{2\alpha_G WiRe}{(1-\beta_{nn})}\Big(Tb_{xy}T_{xy}+Tb_{yy}T_{yy}\Big) = \frac{2(1-\beta_{nn})}{Re}\frac{dv}{dy}, \end{aligned} \tag{2.31}$$

$$T_{yz}+\frac{\varepsilon ReWi}{(1-\beta_{nn})}\Big(Tb_{xx}+Tb_{yy}\Big)T_{yz}+Wi\Bigg(-i\omega T_{yz}+i\alpha UT_{yz}-i\alpha Tb_{xy}w-Tb_{yy}\frac{dw}{dy}+ \\ +\xi\left[\frac{1}{2}T_{xz}\frac{dU}{dy}+\frac{1}{2}Tb_{xy}\left(i\beta u+i\alpha w\right)+\frac{1}{2}Tb_{yy}\left(i\beta v+\frac{dw}{dy}\right)\right]\Bigg)+ \\ +\frac{\alpha_G WiRe}{(1-\beta_{nn})}\Big(Tb_{xy}T_{xz}+Tb_{yy}T_{yz}\Big)=\frac{(1-\beta_{nn})}{Re}\left(\frac{dw}{dy}+i\beta v\right), \tag{2.32}$$

$$T_{zz}+\frac{\varepsilon ReWi}{(1-\beta_{nn})}\Big(Tb_{xx}+Tb_{yy}\Big)T_{zz}+Wi\Big(-i\omega T_{zz}+i\alpha UT_{zz}\Big)=\frac{2i\beta(1-\beta_{nn})}{Re}w. \tag{2.33}$$

For simplicity, the notation $\overline{u}$ has been omitted to denote the disturbances.

The stability analysis is performed by obtaining the solution of the system of equations (2.24) - (2.33). The solution method used in this work is described in chapter 4.

CHAPTER

3

SQUIRE'S THEOREM FOR VISCOELASTIC FLUID FLOWS

This chapter presents an extension of Squire's theorem, first for Newtonian fluid flows. Then, the study presented by Squire (1933) is extended to non-Newtonian fluid flows, considering the analysis of the LPOG constitutive equation for the viscoelastic models UCM, Oldroyd-B, Giesekus, and LPTT.

Squire showed that the stability analysis is sufficient to look only at two-dimensional disturbances for Newtonian fluid flows between parallel plates. From Squire's work, it became clear that three-dimensional disturbances will always be more stable than two-dimensional ones. In other words, the critical Reynolds number for two-dimensional disturbances is smaller than any value for which unstable three-dimensional disturbances exist. This conclusion simplifies the stability analysis considerably, so it is desirable to know which viscoelastic fluid models satisfy this theorem.

Squire (1933) shows this fact using the Orr-Sommerfeld equation for Newtonian fluid flows. In this work, the analysis was reproduced using the conservation equations (2.24) – (2.27) and the constitutive equations (2.28) – (2.33). For this, it is necessary to rewrite the three-dimensional system of equations for the disturbances into an equivalent two-dimensional system through a few changes in the variables of the three-dimensional equation system. Therefore, by mathematical manipulations and changing variables, the three-dimensional (u,v,w) components become $(\overline{u},\overline{v})$, and the three-dimensional tensors component $T_{xx},T_{xy},T_{xz},T_{yy},T_{yz}$ and T_{zz} become $\overline{T}_{xx},\overline{T}_{xy}$ and $\overline{T}_{yy}$. The superscript notation (–) denotes the equivalent two-dimensional transformed variable.

From the three-dimensional continuity equation, we have

$$i\alpha u + i\beta w + \frac{dv}{dy} = 0$$

$$\implies i(\alpha u+\beta w)+\frac{dv}{dy}=0.$$

The following change of variables is proposed:

$$\alpha u+\beta w=\overline{\alpha}\,\overline{u}, \tag{3.1}$$

and

$$v=\overline{v}, \tag{3.2}$$

such that a two-dimensional equivalent continuity equation can be obtained, as follows

$$i\overline{\alpha}\,\overline{u}+\frac{d\overline{v}}{dy}=0. \tag{3.3}$$

For the momentum equations, we start with the changes of variables (3.1) and (3.2). Multiplying α by (2.25) and adding to β multiplied by (2.27), we have

$$\begin{aligned}-i\omega(\alpha u+\beta w)+iU\alpha(\alpha u+\beta w)+\alpha v\frac{dU}{dy}=-i(\alpha^2+\beta^2)p+\\ +\frac{\beta_{nn}}{Re}\left[-(\alpha^2+\beta^2)(\alpha u+\beta w)+\frac{d^2(\alpha u+\beta w)}{dy^2}\right]i\alpha^2T_{xx}+\alpha\frac{dT_{xy}}{dy}+\\ +i\alpha\beta T_{xz}+i\alpha\beta T_{xz}+i\beta^2T_{zz}+\beta\frac{dT_{yz}}{dy}.\end{aligned}$$

Applying the change of variables (3.1) and (3.2) to this equation, results

$$\begin{aligned}-i\omega\overline{\alpha}\,\overline{u}+iU\alpha\overline{\alpha}\,\overline{u}+\alpha\overline{v}\frac{dU}{dy}=-i(\alpha^2+\beta^2)p+\\ +\frac{\beta_{nn}}{Re}\left[-(\alpha^2+\beta^2)\overline{\alpha}\,\overline{u}+\frac{d^2(\overline{\alpha}\,\overline{u})}{dy^2}\right]+i\alpha^2T_{xx}+\alpha\frac{dT_{xy}}{dy}+\\ +i\alpha\beta T_{xz}+i\alpha\beta T_{xz}+i\beta^2T_{zz}+\beta\frac{dT_{yz}}{dy}.\end{aligned} \tag{3.4}$$

Defining, as Squire proposed (SQUIRE, 1933),

$$\overline{\alpha}^2=\alpha^2+\beta^2, \tag{3.5}$$

and applying in equation (3.4), results

$$\begin{aligned}-i\omega\overline{\alpha}\,\overline{u}+iU\alpha\overline{\alpha}\,\overline{u}+\alpha\overline{v}\frac{dU}{dy}=-i\overline{\alpha}^2p+\frac{\beta_{nn}}{Re}\left(-\overline{\alpha}^2\overline{\alpha}\,\overline{u}+\overline{\alpha}\frac{d^2\overline{u}}{dy^2}\right)+\\ +i\alpha^2T_{xx}+\alpha\frac{dT_{xy}}{dy}+i\alpha\beta T_{xz}+i\alpha\beta T_{xz}+i\beta^2T_{zz}+\beta\frac{dT_{yz}}{dy}.\end{aligned}$$

Dividing this equation by α, it is possible to define changes of variables for ω, p and the Reynolds number Re as follows

$$\overline{\omega}=\omega\frac{\overline{\alpha}}{\alpha}, \tag{3.6}$$

$$\overline{p} = p\frac{\overline{\alpha}}{\alpha}, \tag{3.7}$$

and

$$\overline{Re} = Re\frac{\alpha}{\overline{\alpha}}. \tag{3.8}$$

Applying these variable changes in the resulting equation, a two-dimensional equivalent momentum equation in the streamwise direction x is obtained for the three-dimensional disturbances equation

$$\begin{aligned} -i\overline{\omega}\,\overline{u} + iU\overline{\alpha}\,\overline{u} + \overline{v}\frac{dU}{dy} = -i\overline{\alpha}\,\overline{p} + \frac{\beta_{nn}}{\overline{Re}}\left(-\overline{\alpha}^2\,\overline{u} + \frac{d^2\overline{u}}{dy^2}\right) + \\ + i\alpha T_{xx} + \frac{dT_{xy}}{dy} + 2i\beta T_{xz} + i\frac{\beta^2}{\alpha}T_{zz} + \frac{\beta}{\alpha}\frac{dT_{yz}}{dy}, \end{aligned} \tag{3.9}$$

except for the extra-stress tensor components T, which need special treatment.

For the momentum equation in the y direction, multiplying $\overline{\alpha}/\alpha$ by (2.26) and applying the variable changes defined earlier, a two-dimensional equivalent equation for the three-dimensional equation (2.26) is obtained.

$$-i\overline{\omega}\,\overline{v} + iU\overline{\alpha}\,\overline{v} = -\frac{d\overline{p}}{dy} + \frac{\beta_{nn}}{\overline{Re}}\left(-\overline{\alpha}^2\,\overline{v} + \frac{d^2\overline{v}}{dy^2}\right) + i\overline{\alpha}T_{xy} + \frac{\overline{\alpha}}{\alpha}\frac{dT_{yy}}{dy} + i\frac{\overline{\alpha}}{\alpha}\beta T_{yz}. \tag{3.10}$$

For the component of the extra-stress tensor in the equation (3.10), the following changes to the variable can be made as follows

$$\overline{T}_{yy} = \frac{\overline{\alpha}}{\alpha}T_{yy}, \tag{3.11}$$

and

$$\overline{T}_{xy} = \frac{1}{\alpha}\left(\alpha T_{xy} + \beta T_{yz}\right), \tag{3.12}$$

where the equation (3.10) can be rewritten as

$$-i\overline{\omega}\,\overline{v} + iU\overline{\alpha}\,\overline{v} = -\frac{d\overline{p}}{dy} + \frac{\beta_{nn}}{\overline{Re}}\left(-\overline{\alpha}^2\,\overline{v} + \frac{d^2\overline{v}}{dy^2}\right) + i\overline{\alpha}\overline{T}_{xy} + \frac{d\overline{T}_{yy}}{dy}. \tag{3.13}$$

For equation (3.9), the change of variable (3.12) can be used, resulting in

$$\begin{aligned} -i\overline{\omega}\,\overline{u} + iU\overline{\alpha}\,\overline{u} + \overline{v}\frac{dU}{dy} = -i\overline{\alpha}\,\overline{p} + \frac{\beta_{nn}}{\overline{Re}}\left(-\overline{\alpha}^2\,\overline{u} + \frac{d^2\overline{u}}{dy^2}\right) + \\ + i\alpha T_{xx} + 2i\beta T_{xz} + i\frac{\beta^2}{\alpha}T_{zz} + \frac{d\overline{T}_{xy}}{dy}. \end{aligned}$$

Defining the change of variable,

$$\overline{\alpha}\,\overline{T}_{xx} = \frac{1}{\alpha}\left(\alpha^2 T_{xx} + 2\alpha\beta T_{xz} + \beta^2 T_{zz}\right), \tag{3.14}$$

the following equation is obtained

$$-i\overline{\omega}\,\overline{u} + iU\overline{\alpha}\,\overline{u} + \overline{v}\frac{dU}{dy} = -i\overline{\alpha}\,\overline{p} + \frac{\beta_{nn}}{\overline{Re}}\left(-\overline{\alpha}^2\,\overline{u} + \frac{d^2\overline{u}}{dy^2}\right) + i\overline{\alpha}\,\overline{T}_{xx} + \frac{d\overline{T}_{xy}}{dy}. \tag{3.15}$$

Therefore, the equations (3.3), (3.13) and (3.15) are the equivalent system of two-dimensional conservation equations for the three-dimensional disturbances for viscoelastic fluid flows.

Given the transformations in Eqs. (3.1), (3.2), (3.5), (3.6), (3.7), (3.8), (3.11), (3.12), and (3.14) it was possible to derive the equivalent two-dimensional system of equations (3.3), (3.13) and (3.15) for the three-dimensional disturbances for viscoelastic fluid flows.

In the following sections, the different constitutive equations for non-Newtonian viscoelastic fluids will be analyzed to verify if it is possible to arrive at equivalent two-dimensional equations to the three-dimensional disturbance equations for the extra-stress tensor components, Eqs. (2.28) to (2.33). The applicability of Squire's theorem depends on whether these equivalent equations exist.

3.1 Oldroyd-B model

Bistagnino *et al.* (2007) show that Squire's theorem is valid for the Oldroyd-B and UCM models. Using the LPOG constitutive system of equations (2.28)–(2.33), Bistagnino's result may be verified assuming $\varepsilon = \xi = \alpha_G = 0$, resulting in the constitutive equation system for the Oldroyd-B model.

The T_{yy} tensor component equation (2.31), after the simplifications for the Oldroyd-B model, results

$$T_{yy} + Wi\left[-i\omega T_{yy} + + i\alpha U T_{yy} + \frac{dTb_{yy}}{dy}v - 2i\alpha T b_{xy} v - 2Tb_{yy}\frac{dv}{dy}\right] = \\ = \frac{2(1-\beta_{nn})}{Re}\frac{dv}{dy},$$

Applying the changes of variable (3.2), (3.6), (3.8) and (3.11) for $\overline{v}$, $\overline{\omega}$, $\overline{Re}$ and $\overline{T}_{yy}$, respectively, the simplified equation results

$$\frac{\alpha}{\overline{\alpha}}\overline{T}_{yy} + Wi\left[-i\left(\frac{\alpha}{\overline{\alpha}}\right)^2\overline{\omega}\,\overline{T}_{yy} + iU\alpha\frac{\alpha}{\overline{\alpha}}\overline{T}_{yy} + \frac{dTb_{yy}}{dy}\overline{v} - 2Tb_{xy}i\alpha\overline{v} - 2Tb_{yy}\frac{d\overline{v}}{dy}\right] = \\ = \frac{2(1-\beta_{nn})}{\overline{Re}}\frac{\alpha}{\overline{\alpha}}\frac{d\overline{v}}{dy}.$$

Multiplying both sides of the equation by $\overline{\alpha}/\alpha$, we have

$$\overline{T}_{yy}+Wi\frac{\overline{\alpha}}{\alpha}\left[-i\left(\frac{\alpha}{\overline{\alpha}}\right)^2\overline{\omega}\,\overline{T}_{yy}+iU\alpha\frac{\alpha}{\overline{\alpha}}\overline{T}_{yy}+\frac{dTb_{yy}}{dy}\overline{v}-2Tb_{xy}i\alpha\overline{v}-2Tb_{yy}\frac{d\overline{v}}{dy}\right]= \\ =\frac{2(1-\beta_{nn})}{\overline{Re}}\frac{d\overline{v}}{dy},$$

then,

$$\overline{T}_{yy}+Wi\left[-i\left(\frac{\alpha}{\overline{\alpha}}\right)\overline{\omega}\,\overline{T}_{yy}+iU\alpha\overline{T}_{yy}+\frac{\overline{\alpha}}{\alpha}\frac{dTb_{yy}}{dy}\overline{v}-2Tb_{xy}i\alpha\frac{\overline{\alpha}}{\alpha}\overline{v}-2\frac{\overline{\alpha}}{\alpha}Tb_{yy}\frac{d\overline{v}}{dy}\right]= \\ =\frac{2(1-\beta_{nn})}{\overline{Re}}\frac{d\overline{v}}{dy}.$$

Or,

$$\overline{T}_{yy}+Wi\frac{\alpha}{\overline{\alpha}}\left[-i\overline{\omega}\,\overline{T}_{yy}+iU\overline{\alpha}\overline{T}_{yy}+\left(\frac{\overline{\alpha}}{\alpha}\right)^2\frac{dTb_{yy}}{dy}\overline{v}-2i\overline{\alpha}Tb_{xy}\frac{\overline{\alpha}}{\alpha}\overline{v}+ \right. \\ \left. -2\left(\frac{\overline{\alpha}}{\alpha}\right)^2Tb_{yy}\frac{d\overline{v}}{dy}\right]=\frac{2(1-\beta_{nn})}{\overline{Re}}\frac{d\overline{v}}{dy}.$$

Defining the following changes of variables for the Weissenberg number and the baseflow stress tensor components,

$$\overline{Wi}=\frac{\alpha}{\overline{\alpha}}Wi, \tag{3.16}$$

$$\overline{Tb}_{xy}=\frac{\overline{\alpha}}{\alpha}Tb_{xy}, \tag{3.17}$$

and

$$\overline{Tb}_{yy}=\left(\frac{\overline{\alpha}}{\alpha}\right)^2Tb_{yy}, \tag{3.18}$$

a two-dimensional equivalent constitutive equation it is obtained for the tensor component $\overline{T}_{yy}$,

$$\overline{T}_{yy}+\overline{Wi}\left(-i\overline{\omega}\,\overline{T}_{yy}+iU\overline{\alpha}\overline{T}_{yy}+\frac{d\overline{Tb}_{yy}}{dy}\overline{v}-2i\overline{\alpha}\overline{Tb}_{xy}\overline{v}-2\overline{Tb}_{yy}\frac{d\overline{v}}{dy}\right)= \\ =\frac{2(1-\beta_{nn})}{\overline{Re}}\frac{d\overline{v}}{dy}. \tag{3.19}$$

For the T_{xy} and T_{yz} tensor components, equations (2.29) and (2.32), the transformation given by (3.12) will be used. Rearranging the original equations for T_{xy} and T_{yz} according to (3.12),

$$\alpha T_{xy}+\alpha Wi\left(-i\omega T_{xy}+i\alpha UT_{xy}-i\alpha Tb_{xx}v+i\beta Tb_{xy}w+\frac{dTb_{xy}}{dy}v-\frac{dU}{dy}T_{yy}+ \right. \\ \left. -Tb_{yy}\frac{du}{dy}\right)+\beta T_{yz}+\beta Wi\left(-i\omega T_{yz}+i\alpha UT_{yz}-i\alpha Tb_{xy}w-Tb_{yy}\frac{dw}{dy}+\right)= \\ =\alpha\frac{(1-\beta_{nn})}{Re}\left(\frac{du}{dy}+i\alpha v\right)+\beta\frac{(1-\beta_{nn})}{Re}\left(\frac{dw}{dy}+i\beta v\right).$$

After additional manipulations,

$$\alpha T_{xy}+\beta T_{yz}+\alpha Wi\left(-i\omega T_{xy}+i\alpha U T_{xy}-i\alpha T b_{xx}v+i\beta T b_{xy}w+\frac{dTb_{xy}}{dy}v+\right.$$
$$\left.-\frac{dU}{dy}T_{yy}-Tb_{yy}\frac{du}{dy}\right)+\beta Wi\left(-i\omega T_{yz}+i\alpha U T_{yz}-i\alpha T b_{xy}w-Tb_{yy}\frac{dw}{dy}+\right)=$$
$$=\frac{(1-\beta_{nn})}{Re}\left(\alpha\frac{du}{dy}+\beta\frac{dw}{dy}+i\alpha^2v+i\beta^2v\right).$$

Applying the proposed changes of variables for Wi, Tb_{xy} and Tb_{yy},

$$\alpha\overline{T}_{xy}+Wi\left(-i\omega\alpha\overline{T}_{xy}+i\alpha^2U\overline{T}_{xy}-i\alpha^2Tb_{xx}\overline{v}+\alpha\frac{dTb_{xy}}{dy}\overline{v}+\right.$$
$$\left.-\alpha\frac{dU}{dy}T_{yy}-\overline{\alpha}Tb_{yy}\frac{d\overline{u}}{dy}\right)=\frac{(1-\beta_{nn})}{\overline{Re}}\frac{\alpha}{\overline{\alpha}}\left(\overline{\alpha}\frac{d\overline{u}}{dy}+i\overline{\alpha}^2\overline{v}\right),$$

or,

$$\overline{T}_{xy}+Wi\left(-i\omega\overline{T}_{xy}+i\alpha U\overline{T}_{xy}-i\alpha Tb_{xx}\overline{v}+\frac{dTb_{xy}}{dy}\overline{v}+\right.$$
$$\left.-\frac{dU}{dy}T_{yy}-\frac{\overline{\alpha}}{\alpha}Tb_{yy}\frac{d\overline{u}}{dy}\right)=\frac{(1-\beta_{nn})}{\overline{Re}}\left(\frac{d\overline{u}}{dy}+i\overline{\alpha}\overline{v}\right).$$

Using the transformation proposed for the Weissenberg number and the frequency,

$$Wi=\overline{Wi}\frac{\overline{\alpha}}{\alpha},$$

and

$$\omega=\overline{\omega}\frac{\alpha}{\overline{\alpha}},$$

the resulting equation for the stress tensor becomes

$$\overline{T}_{xy}+\overline{Wi}\left[-i\overline{\omega}\overline{T}_{xy}+i\overline{\alpha}U\overline{T}_{xy}-i\overline{\alpha}Tb_{xx}\overline{v}+\frac{\overline{\alpha}}{\alpha}\frac{dTb_{xy}}{dy}\overline{v}+\right.$$
$$\left.-\frac{\overline{\alpha}}{\alpha}\frac{dU}{dy}T_{yy}-\left(\frac{\overline{\alpha}}{\alpha}\right)^2Tb_{yy}\frac{d\overline{u}}{dy}\right]=\frac{(1-\beta_{nn})}{\overline{Re}}\left(\frac{d\overline{u}}{dy}+i\overline{\alpha}\overline{v}\right).$$

Defining the following change of variable for the base flow stress component Tb_{xx}

$$Tb_{xx}=\overline{Tb}_{xx}, \tag{3.20}$$

and using the variable changes already defined, the equation for $\overline{T}_{xy}$ results

$$\overline{T}_{xy}+\overline{Wi}\left(-i\overline{\omega}\overline{T}_{xy}+i\overline{\alpha}U\overline{T}_{xy}-i\overline{\alpha}\overline{Tb}_{xx}\overline{v}+\frac{d\overline{Tb}_{xy}}{dy}\overline{v}+\right.$$
$$\left.-\frac{dU}{dy}\overline{T}_{yy}-\overline{Tb}_{yy}\frac{d\overline{u}}{dy}\right)=\frac{(1-\beta_{nn})}{\overline{Re}}\left(\frac{d\overline{u}}{dy}+i\overline{\alpha}\overline{v}\right), \tag{3.21}$$

which is the equivalent two-dimensional equation for the T_{xy} tensor component.

Finally, to verify that Squire's theorem is valid for the Oldroyd-B model, it remains to show that using the transformations defined previously, the transformation proposed in equation (3.14), an equivalent two-dimensional equation is obtained. Adding equations (2.28), (2.30) and (2.33), according to (3.14), results

$$\begin{aligned}
&(\alpha^2 T_{xx} + 2\alpha\beta T_{xz} + \beta^2 T_{zz}) + Wi\alpha^2 \Bigg(-i\omega T_{xx} + i\alpha U T_{xx} - 2i\alpha T b_{xx} u + \\
&+ \frac{dTb_{xx}}{dy} v - 2\frac{dU}{dy} T_{xy} - 2Tb_{xy}\frac{du}{dy} \Bigg) + 2Wi\alpha\beta \Bigg(-i\omega T_{xz} + i\alpha U T_{xz} + \\
&- i\alpha T b_{xx} w - Tb_{xy}\frac{dw}{dy} - \frac{dU}{dy} T_{yz} \Bigg) + Wi\beta^2 \left(-i\omega T_{zz} + i\alpha U T_{zz}\right) = \\
&= \alpha^2 \frac{2i\alpha(1-\beta_{nn})}{Re} u + 2\alpha\beta \frac{(1-\beta_{nn})}{Re} (i\beta u + i\alpha w) + \beta^2 \frac{2i\beta(1-\beta_{nn})}{Re} w,
\end{aligned}$$

Rewriting,

$$\begin{aligned}
&\overline{\alpha}\alpha \overline{T}_{xx} + Wi \Bigg(-i\omega\overline{\alpha}\alpha \overline{T}_{xx} + i\overline{\alpha}\alpha^2 U \overline{T}_{xx} - 2i\alpha^3 T b_{xx} u + \alpha^2 \frac{dTb_{xx}}{dy} v + \\
&-2\alpha^2 \frac{dU}{dy} T_{xy} - 2\alpha^2 Tb_{xy}\frac{du}{dy} \Bigg) + Wi \Bigg(-2i\alpha^2\beta T b_{xx} w - 2\alpha\beta T b_{xy}\frac{dw}{dy} + \\
&-2\alpha\beta\frac{dU}{dy} T_{yz} \Bigg) = \alpha^2 \frac{2i\alpha(1-\beta_{nn})}{Re} u + 2\alpha\beta \frac{(1-\beta_{nn})}{Re} (i\beta u + i\alpha w) + \\
&+ \beta^2 \frac{2i\beta(1-\beta_{nn})}{Re} w.
\end{aligned}$$

Dividing the resulting equation by $\overline{\alpha}\alpha$, we have

$$\begin{aligned}
&\overline{T}_{xx} + Wi \Bigg(-i\omega \overline{T}_{xx} + i\alpha U \overline{T}_{xx} - 2i\frac{\alpha^2}{\overline{\alpha}} T b_{xx} u + \frac{\alpha}{\overline{\alpha}}\frac{dTb_{xx}}{dy} v - 2\frac{\alpha}{\overline{\alpha}}\frac{dU}{dy} T_{xy} + \\
&-2\frac{\alpha}{\overline{\alpha}} Tb_{xy}\frac{du}{dy} \Bigg) + Wi \Bigg(-2i\frac{\alpha}{\overline{\alpha}}\beta T b_{xx} w - 2\frac{1}{\overline{\alpha}}\beta T b_{xy}\frac{dw}{dy} - 2\frac{1}{\overline{\alpha}}\beta\frac{dU}{dy} T_{yz} \Bigg) = \\
&= \frac{\alpha}{\overline{\alpha}}\frac{2i\alpha(1-\beta_{nn})}{Re} u + 2\frac{1}{\overline{\alpha}}\beta\frac{(1-\beta_{nn})}{Re} (i\beta u + i\alpha w) + \beta^2 \frac{1}{\alpha\overline{\alpha}}\frac{2i\beta(1-\beta_{nn})}{Re} w.
\end{aligned}$$

Replacing $\overline{Wi}$ and $\overline{Re}$ and manipulating the terms in the equation, we have

$$\begin{aligned}
&\overline{T}_{xx} + \overline{Wi}\frac{\overline{\alpha}}{\alpha} \Bigg(-i\omega \overline{T}_{xx} + i\alpha U \overline{T}_{xx} - 2i\frac{\alpha^2}{\overline{\alpha}} T b_{xx} u + \frac{\alpha}{\overline{\alpha}}\frac{dTb_{xx}}{dy} v - 2\frac{\alpha}{\overline{\alpha}}\frac{dU}{dy} T_{xy} + \\
&-2\frac{\alpha}{\overline{\alpha}} Tb_{xy}\frac{du}{dy} \Bigg) + \overline{Wi}\frac{\overline{\alpha}}{\alpha} \Bigg(-2i\frac{\alpha}{\overline{\alpha}}\beta T b_{xx} w - 2\frac{1}{\overline{\alpha}}\beta T b_{xy}\frac{dw}{dy} - 2\frac{1}{\overline{\alpha}}\beta\frac{dU}{dy} T_{yz} \Bigg) = \\
&= \frac{2(1-\beta_{nn})}{\overline{Re}}\frac{\alpha}{\overline{\alpha}^2} \left(i\alpha^2 u + i\beta\alpha w + i\beta^2 u + i\frac{\beta^2}{\alpha} w \right).
\end{aligned}$$

Substituting $\overline{\omega}$ in the resulting equation and using $\alpha u+\beta w$, we then have

$$\overline{T}_{xx}+\overline{Wi}\frac{\overline{\alpha}}{\alpha}\left(-i\overline{\omega}\frac{\alpha}{\overline{\alpha}}\overline{T}_{xx}+i\alpha U\overline{T}_{xx}-2i\frac{\alpha^2}{\overline{\alpha}}Tb_{xx}u+\frac{\alpha}{\overline{\alpha}}\frac{dTb_{xx}}{dy}v-2\frac{\alpha}{\overline{\alpha}}\frac{dU}{dy}T_{xy}+\right.$$
$$\left.-2\frac{\alpha}{\overline{\alpha}}Tb_{xy}\frac{du}{dy}\right)+\overline{Wi}\frac{\overline{\alpha}}{\alpha}\left(-2i\frac{\alpha}{\overline{\alpha}}\beta Tb_{xx}w-2\frac{1}{\overline{\alpha}}\beta Tb_{xy}\frac{dw}{dy}-2\frac{1}{\overline{\alpha}}\beta\frac{dU}{dy}T_{yz}\right)=$$
$$=\frac{2(1-\beta_{nn})}{\overline{Re}}\frac{\alpha}{\overline{\alpha}^2}\left[i\alpha(\alpha u+\beta w)+i\beta^2\frac{1}{\alpha}(\alpha u+\alpha w)\right].$$

Simplifying the resulting equation, we have

$$\overline{T}_{xx}+\overline{Wi}\left(-i\overline{\omega}\overline{T}_{xx}+i\overline{\alpha}U\overline{T}_{xx}-2i\alpha Tb_{xx}u+\frac{dTb_{xx}}{dy}v-2\frac{dU}{dy}T_{xy}+\right.$$
$$\left.-2Tb_{xy}\frac{du}{dy}\right)+\overline{Wi}\left(-2i\beta Tb_{xx}w-2\frac{\beta}{\alpha}Tb_{xy}\frac{dw}{dy}-2\frac{\beta}{\alpha}\frac{dU}{dy}T_{yz}\right)=$$
$$=\frac{2(1-\beta_{nn})}{\overline{Re}}\frac{\alpha}{\overline{\alpha}^2}\left(i\alpha\overline{\alpha}\overline{u}+i\beta^2\frac{1}{\alpha}\overline{\alpha}\overline{u}\right).$$

Applying the transformations defined earlier, after mathematical manipulations to organize the terms, we have

$$\overline{T}_{xx}+\overline{Wi}\left(-i\overline{\omega}\overline{T}_{xx}+i\overline{\alpha}U\overline{T}_{xx}-2i\overline{\alpha}\overline{Tb}_{xx}\overline{u}+\frac{d\overline{Tb}_{xx}}{dy}\overline{v}-2\frac{dU}{dy}\overline{T}_{xy}+\right.$$
$$\left.-2\frac{\overline{\alpha}}{\alpha}Tb_{xy}\frac{d\overline{u}}{dy}\right)=\frac{2(1-\beta_{nn})}{\overline{Re}}\frac{1}{\overline{\alpha}^2}i\overline{\alpha}\overline{u}\left(\alpha^2+\beta^2\right).$$

Finally, applying the last transformations to the resulting equation and simplifying the terms, results

$$\overline{T}_{xx}+\overline{Wi}\left(-i\overline{\omega}\overline{T}_{xx}+i\overline{\alpha}U\overline{T}_{xx}-2i\overline{\alpha}\overline{Tb}_{xx}\overline{u}+\frac{d\overline{Tb}_{xx}}{dy}\overline{v}-2\frac{dU}{dy}\overline{T}_{xy}+\right.$$
$$\left.-2\overline{Tb}_{xy}\frac{d\overline{u}}{dy}\right)=\frac{2(1-\beta_{nn})}{\overline{Re}}i\overline{\alpha}\,\overline{u},\tag{3.22}$$

which is the equivalent two-dimensional equation for the T_{xx} tensor component. This shows that Squire's theorem is valid for the Oldroyd-B model and also for the UCM model, which is a simplification of the Oldroyd-B when $\beta_{nn}=0$.

3.2 Giesekus model

To verify the validity of Squire's theorem for other models using the LPOG constitutive equation, we have to assign the value of 0 to the unwanted model constant and analyze the resulting equation for the desired model. For the Giesekus model $\varepsilon=\xi=0$ is considered in the LPOG system of equations (2.28) to (2.33).

To verify the validity of Squire's theorem for the Giesekus model, we note that all the tensor components are identical to the terms in the Oldroyd-B model, except for the terms

multiplied by α_G. This additional term corresponds to an anisotropic correction (CASTILLO; WILSON, 2017). Therefore, it is necessary to show that these additional terms also result in equivalent two-dimensional terms.

Making the combination of the extra terms according to the transformation given by equation (3.14), we have

$$\frac{1}{\alpha}\left[\alpha^2\frac{2\alpha_G WiRe}{(1-\beta_{nn})}\left(Tb_{xx}T_{xx}+Tb_{xy}T_{xy}\right)+2\alpha\beta\frac{\alpha_G WiRe}{(1-\beta_{nn})}\left(Tb_{xx}T_{xz}+Tb_{xy}T_{yz}\right)\right],$$

rewriting,

$$\frac{\alpha_G WiRe}{(1-\beta_{nn})}\frac{1}{\alpha}\left[2Tb_{xx}\left(\alpha^2T_{xx}+\alpha\beta T_{xz}\right)+2Tb_{xy}\left(\alpha^2T_{xy}+\alpha\beta T_{yz}\right)\right],$$

or

$$\frac{\alpha_G WiRe}{(1-\beta_{nn})}\left[2Tb_{xx}\frac{1}{\alpha}\left(\alpha^2T_{xx}+\alpha\beta T_{xz}\right)+2Tb_{xy}\left(\alpha T_{xy}+\beta T_{yz}\right)\right].$$

Applying transformation (3.12) to the last term, we have

$$\frac{\alpha_G WiRe}{(1-\beta_{nn})}\left[2Tb_{xx}\frac{1}{\alpha}\left(\alpha^2T_{xx}+\alpha\beta T_{xz}\right)+2Tb_{xy}\alpha\overline{T}_{xy}\right],$$

or, for the base flow tensor terms, using the transformation for Tb_{xy}, Tb_{xx}, Re and Wi

$$\frac{\alpha_G\overline{WiRe}}{(1-\beta_{nn})}\left[2\frac{\overline{\alpha}^2}{\alpha^2}\overline{Tb}_{xx}\left(\alpha T_{xx}+\beta T_{xz}\right)+2\overline{\alpha}\overline{Tb}_{xy}\overline{T}_{xy}\right].$$

However, for the first term between brackets, it is not possible to apply the transformation to obtain $\overline{T}_{xx}$. The equation (2.33) does not have a component associated with α_G such that we could apply the transformation given by (3.14). It shows that the needed transformation for the validity of Squire's theorem considering the Giesekus model is not applicable.

Likewise, it is easy to see that the other transformations fail when considering this model. For example, considering now the transformation (3.12), we have

$$\frac{1}{\alpha}\left[\alpha\frac{\alpha_G WiRe}{(1-\beta_{nn})}\left(Tb_{xy}(T_{xx}+T_{yy})+T_{xy}(Tb_{xx}+Tb_{yy})\right)+\right.$$
$$\left.+\beta\frac{\alpha_G WiRe}{(1-\beta_{nn})}\left(Tb_{xy}T_{xz}+Tb_{yy}T_{yz}\right)\right]$$

$$\Longrightarrow\ \frac{\alpha_G WiRe}{(1-\beta_{nn})}\frac{1}{\alpha}\left\{\alpha\left[Tb_{xy}(T_{xx}+T_{yy})+T_{xy}(Tb_{xx}+Tb_{yy})\right]+\right.$$
$$\left.+\beta\left(Tb_{xy}T_{xz}+Tb_{yy}T_{yz}\right)\right\}$$

$$\Longrightarrow \frac{\alpha_G WiRe}{(1-\beta_{nn})}\frac{1}{\alpha}\left[Tb_{xy}(\alpha T_{xx}+\beta T_{xz}+\alpha T_{yy})+\right.$$
$$\left.+\alpha T_{xy}(Tb_{xx}+Tb_{yy})+\beta Tb_{yy}T_{yz}\right]$$

$$\Longrightarrow \frac{\alpha_G WiRe}{(1-\beta_{nn})}\left[Tb_{xy}\frac{1}{\alpha}(\alpha T_{xx}+\beta T_{xz})+\alpha\frac{1}{\alpha}Tb_{xy}T_{yy}+\right.$$
$$\left.+\frac{1}{\alpha}Tb_{yy}(\alpha T_{xy}+\beta T_{yz})+\alpha\frac{1}{\alpha}Tb_{xx}T_{xy}\right]$$

$$\Longrightarrow \frac{\alpha_G \overline{WiRe}}{(1-\beta_{nn})}\left[\frac{\overline{\alpha}}{\alpha^2}\overline{Tb}_{xy}(\alpha T_{xx}+\beta T_{xz})+\overline{Tb}_{xy}\overline{T}_{yy}+\right.$$
$$\left.+\frac{\overline{\alpha}}{\alpha}\overline{Tb}_{yy}\overline{T}_{xy}+\frac{\overline{\alpha}^2}{\alpha^2}\overline{Tb}_{xx}T_{xy}\right].$$

As can be observed in the resulting equation, the transformations are not satisfied by the equations of the Giesekus model. Therefore, it can be stated that Squire's theorem is not valid for the Giesekus viscoelastic model, confirming the assertion made by Blonce (1997).

3.3 LPTT model

For the LPTT model, the simplification $\alpha_G = 0$ is assumed in the LPOG system of equations (2.28) to (2.33). As done for the Giesekus model, the terms common with the Oldroyd-B model have already been checked for the validity of Squire's theorem, resting only to show the validity (or not) of the transformation for the remaining terms. For the LPTT model, there are two additional dimensionless model constants, ε and ξ.

Starting with the terms associated with ε and applying the transformation (3.14) to obtain an equation for $\overline{T}_{xx}$, we have:

$$+\frac{1}{\alpha}\left\{\alpha^2\left[\frac{\varepsilon ReWi}{(1-\beta_{nn})}(T_{xx}+T_{yy}+T_{zz})Tb_{xx}+\frac{\varepsilon ReWi}{(1-\beta_{nn})}(Tb_{xx}+Tb_{yy})T_{xx}\right]+\right.$$
$$\left.+2\alpha\beta\frac{\varepsilon ReWi}{(1-\beta_{nn})}(Tb_{xx}+Tb_{yy})T_{xz}+\beta^2\frac{\varepsilon ReWi}{(1-\beta_{nn})}(Tb_{xx}+Tb_{yy})T_{zz}\right\}$$

$$\Longrightarrow \frac{\varepsilon ReWi}{(1-\beta_{nn})}\frac{1}{\alpha}\left\{\alpha^2\left[(T_{xx}+T_{yy}+T_{zz})Tb_{xx}+(Tb_{xx}+Tb_{yy})T_{xx}\right]+\right.$$
$$\left.+2\alpha\beta(Tb_{xx}+Tb_{yy})T_{xz}+\beta^2(Tb_{xx}+Tb_{yy})T_{zz}\right\}$$

$$\Longrightarrow \frac{\varepsilon ReWi}{(1-\beta_{nn})}\frac{1}{\alpha}\left[\left(\alpha^2 T_{xx}+\alpha^2 T_{zz}+\alpha^2 T_{xx}+2\alpha\beta T_{xz}+\beta^2 T_{zz}\right)Tb_{xx}+\right.$$
$$\left.+\left(\alpha^2 T_{xx}+2\alpha\beta T_{xz}+\beta^2 T_{zz}\right)Tb_{yy}+\alpha^2 Tb_{xx}T_{yy}\right].$$

Applying the change variables defined earlier, we have

$$\frac{\varepsilon ReWi}{(1-\beta_{nn})}\left[\overline{\alpha}Tb_{xx}\overline{T}_{xx}+\frac{1}{\alpha}\left(\alpha^2 T_{zz}+\alpha^2 T_{xx}\right)Tb_{xx}+\right.$$
$$\left.+\overline{\alpha}Tb_{yy}\overline{T}_{xy}+\alpha Tb_{xx}T_{yy}\right]$$

$$\Longrightarrow \frac{\varepsilon ReWi}{(1-\beta_{nn})}\left[\overline{\alpha}Tb_{xx}\overline{T}_{xx}+\overline{\alpha}Tb_{yy}\overline{T}_{xy}+\alpha\left(T_{xx}+T_{yy}+T_{zz}\right)Tb_{xx}\right]$$

$$\Longrightarrow \frac{\varepsilon\overline{ReWi}}{(1-\beta_{nn})}\left[\frac{\overline{\alpha}^3}{\alpha^2}\overline{Tb}_{xx}\overline{T}_{xx}+\overline{\alpha}\overline{Tb}_{yy}\overline{T}_{xx}+\frac{\overline{\alpha}^2}{\alpha}\left(T_{xx}+T_{zz}\right)\overline{Tb}_{xx}+\overline{\alpha}\overline{Tb}_{xx}\overline{T}_{yy}\right].$$

One can observe that this term of the LPTT model does not satisfy the transformations to obtain the equivalent two-dimensional equation. Therefore, Squire's theorem is not valid for the LPTT viscoelastic model.

The common aspect between the Giesekus and LPTT models is the parameters associated with anisotropy. These terms introduce spanwise dependence on the constitutive equation that cannot be reduced to a two-dimensional equivalent form. Others anisotropic non-Newtonian models may fail to allow a transformation of variables leading to Squire's theorem.

Hence, the need arises to perform stability analysis for three-dimensional flows for these viscoelastic models, as the two-dimensional analysis does not guarantee that three-dimensional disturbances are more stable, as stated in Squire's theorem.

This chapter was published in Furlan *et al.* (2022).

CHAPTER

4

SOLUTION METHODS FOR THE STABILITY PROBLEM

This chapter describes the solution method for the stability analysis problem of three-dimensional fluid flow for viscoelastic fluids considering the system of equations (2.24) - (2.33).

To solve the stability analysis problem, it is necessary to the previous solution of the laminar flow. Section 4.1 presents the solution of the baseflow for the viscoelastic fluid flows considered in this work.

To solve the system (2.24) - (2.33) and therefore to obtain information about the stability of the fluid flow, it was adopted the matrix method for the eigenvalue problem. This solution method is described in Section 4.2.

4.1 Laminar Flow

Linear stability theory uses the decomposition hypothesis for the instantaneous flow, which decomposes into laminar flow and disturbances.

The viscoelastic models used in this work adopted results references that present solutions for laminar flow between parallel plates. It is worth noting that the laminar flow is two-dimensional due to the assumptions of fluid flow applied.

For the UCM and Oldroyd-B models, the solution for the laminar flow components is achieved analytically, as presented in Brandi, Mendonça and Souza (2019). For these models, the analytical components are calculated from the wall-normal coordinate to the flow (y),

$$U(y) = 1 - y^2, \tag{4.1}$$

$$Tb_{xx}(y) = 8Wi\frac{(1-\beta_{nn})}{Re}y^2, \tag{4.2}$$

$$Tb_{xy}(y) = -2\frac{(1-\beta_{nn})}{Re}y, \tag{4.3}$$

and

$$Tb_{yy}(y) = 0. \tag{4.4}$$

For the Giesekus model, the reference Furlan *et al.* (2021) was used as a script for the laminar flow calculation. When the purely polymeric flow is considered, the reference's formulation *(3.1)* was adopted. When it is considered solvent in the viscoelastic fluid mixture, the formulation *(3.2)* from the reference was adopted.

For the LPTT model, the reference Alves, Pinho and Oliveira (2001) was used for the laminar flow, considering the purely polymeric LPTT fluid flow. When a solvent is considered in the viscoelastic fluid mixture, a semi-analytical solution was developed and published in Araujo *et al.* (2022).

4.2 Matrix Method

The matrix method consists of rewriting the system of equations (2.24) - (2.33) and solving the eigenvalue problem associated with the stability analysis. Therefore, from the system of equations obtained by applying linear stability theory to stability analysis, one rewrites the system of equations in the form of an eigenvalue problem for the desired analysis (temporal or spatial).

In this work, the spatial analysis of the disturbances was performed by analyzing the spatial amplification rate α_i.

Rewriting the system of equations in matrix form, as follows

$$LV = \alpha FV, \tag{4.5}$$

for the eigenvector V,

$$V = [u,\ \alpha u,\ v,\ \alpha v,\ w,\ \alpha w,\ p,\ T_{xx},\ T_{xy},\ T_{xz},\ T_{yy},\ T_{yz},\ T_{zz}], \tag{4.6}$$

it is possible to solve the stability analysis problem by finding the eigenvalue α (or ω for the time analysis), using some method (direct or iterative) for calculating the eigenvalue. In this work, MATLAB software was used to implement the stability analysis code, the laminar flow for each desired model, and to obtain the solution of the matrix equation (4.5), the software's pre-programmed function EIG was used. The EIG function automatically selects the optimal algorithm based on the properties of the matrices L and F. For Hermitian L and positive definite Hermitian F, the eigenvalues are calculated via the Cholesky factorization of F. Otherwise, Schur's decomposition is used, which ignores the symmetry of L and F. The derivatives accompanying the amplitudes of the fluctuations are approximated using Chebyshev polynomials as

suggested by Don and Solomonoff (1995) and implemented in Weideman and Reddy (2000), <http://www.lmm.jussieu.fr/~hoepffner/phdcodes/chebdif.m>accessed in 06/21/2022.

Details about the matrices L and F and their coefficients are given in Appendix A.

The boundary conditions imposed for the velocities of the disturbances u, v and w are of the no-slip type on the channel walls.

4.3 Spatial and Temporal Analysis of Instabilities

The solution of the 4.5 corresponds to an eigenvalue problem, solution exists for some values of the parameters $\alpha, \omega, \beta, Re, \beta_{nn}, Wi, \alpha_G, \varepsilon$ and ξ, and depends on the velocity profile of the flow in question. The disturbances analyzed here are non-stationary and propagate as Tollmien-Schlichting waves.

When ω is a real number and α is a complex number, the amplitude of the disturbance can increase, decrease, or be neutral in the direction of laminar flow. Under these conditions, the formulation is called a spatial formulation. The components ω_r, α_r and α_i represent the frequency, the wavenumber and the spatial amplification rate, respectively. For the temporal formulation, α is a real number, and ω is a complex number. The components ω_r, ω_i and α_r represent the frequency, the temporal amplification rate and the wavenumber, respectively.

Table 1 presents the classification of instabilities using temporal and spatial analyses.

Table 1 – Classification of Instabilities.

Analysis type	amplification rate	amplitude	classification
temporal analysis	$\omega_i < 0$	decreases	stable
	$\omega_i = 0$	constant	neutral
	$\omega_i > 0$	increases	unstable
spatial analysis	$\alpha_i < 0$	increases	unstable
	$\alpha_i = 0$	constant	neutral
	$\alpha_i > 0$	decreases	stable

CHAPTER

5

RESULTS

This chapter presents the results obtained for stability analysis for three-dimensional viscoelastic flows by the method presented in this work.

For each viscoelastic model, the validation/verification of the results was performed using the results presented in the literature. In general, the literature results are for two-dimensional flows. For the Oldroyd-B and UCM model, as shown in Chapter 3, it is possible to validate the three-dimensional results using Squire's theorem. For the Giesekus and LPTT models, Squire's theorem is not valid, and no results for stability analysis of these models considering three-dimensional flows were found in the literature.

The neutral stability curves of this work were built considering the variation of the Reynolds number on the x axis by the frequency on the y axis (in the images denoted as ω_z).

For all simulations performed, 150 Chebyshev polynomials were considered. This number was estimated using some convergence tests. For some cases, reasonably good results were obtained using 80 or 100 polynomials, but 150 was stipulated for all simulations to obtain the same accuracy in all simulations.

5.1 Oldroyd-B and UCM models

This section presents the results obtained for stability analysis of the Oldroyd-B and UCM viscoelastic models for three-dimensional flow.

To verify the results obtained, Table 2 presents comparisons between literature results for stability analysis of two-dimensional Oldroyd-B fluid flow presented in Brandi, Mendonça and Souza (2019) and the results obtained using the method presented in this work. This comparison is performed using the amplification rate α_i obtained by solving the system (4.5).

From Table 2, it can be seen that the results obtained by the presented method are

Table 2 – Comparison between the amplification rate present in the literature and the results obtained in this work.

Case	Re	β_{nn}	Wi	ω	Ref. DNS α_i	Ref. LST α_i	Pres. work α_i
A	6500	1.0	0.0	0.250	-2.60×10^{-3}	-2.68×10^{-3}	-2.6828×10^{-3}
B	6500	0.9	10.0	0.400	8.32×10^{-2}	8.32×10^{-2}	8.3054×10^{-2}
C	8000	0.9	5.0	0.240	-9.00×10^{-3}	-9.00×10^{-3}	-9.2293×10^{-3}
D	5200	0.9	1.0	0.200	2.08×10^{-2}	2.02×10^{-2}	2.0635×10^{-2}
E	6500	0.7	10.0	0.276	-3.50×10^{-3}	-3.60×10^{-3}	-3.6947×10^{-3}

The results of the present work were performed using 150 Chebyshev modes.

satisfactory when compared to the results found in the literature.

Figure 1 presents comparisons for the neutral stability curves for the Oldroyd-B fluid flow by varying the solvent β_{nn} contribution in the fluid mixture and the Weissenberg number Wi in the simulations.

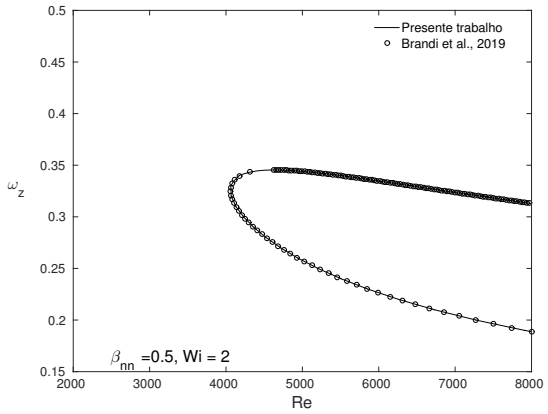

(a) Neutral Curve for $\beta_{nn} = 0.5$ and $Wi = 2$

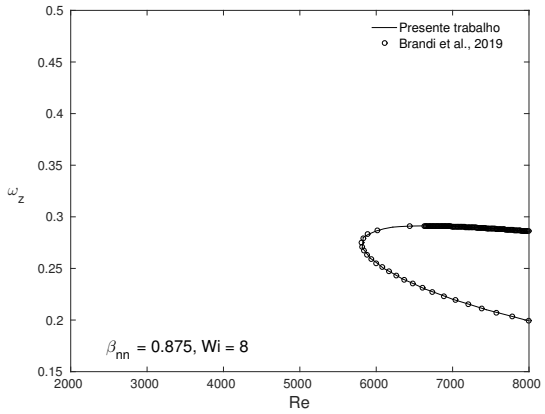

(b) Neutral Curve for $\beta_{nn} = 0.875$ and $Wi = 8$

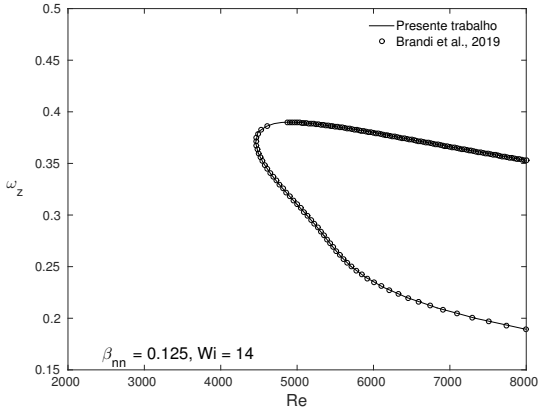

(c) Neutral Curve for $\beta_{nn} = 0.125$ and $Wi = 14$

Figure 1 – Comparison of neutral curves presented in the literature and the results obtained in this work.

Source: Elaborated by the author.

It can be seen that the neutral curves are in agreement, showing that the solution method for the stability problem presented here works for constructing the neutral stability curves.

To verify the stability analysis results for three-dimensional flows, the results presented in Table 2 were used, considering values for the variable β (for two-dimensional flows, $\beta = 0$) using the relations presented in Chapter 3.

For case B of Table 2, we have the value

$$\overline{\alpha} = 1.36979264761636 + 0.0830546458400634i.$$

Using the relation (3.5), the expected value for the eigenvalue α considering a three-dimensional flow is obtained.

Making $\beta = 0.2$, the value of α for the expected three-dimensional flow, by Squire's relation is

$$\alpha = 1.35516846947716 + 0.0839509225491296i.$$

Making the variable changes in the code for ω, Re and Wi from the two-dimensional one to find the equivalent three-dimensional value through their respective transformations, and solving the three-dimensional stability problem for this case, the following value is obtained

$$\alpha = 1.35516846948083 + 0.0839509225400766i.$$

The three-dimensional values for the flow variables are:

$$\omega = 0.395760974060906 + 0.000518751128458257i,$$

$$Re = 6569.61070777306 - 8.611240601162 05i$$

and

$$Wi = 10.1070933965739 - 0.0132480624633262i.$$

It is possible to see that the values of the amplification rates are very close, with a difference to the eleventh decimal place.

5.1.1 UCM Results

Here, the results for stability analysis are presented, considering the UCM model as the constitutive model for the viscoelastic fluid flow. Neutral stability curves are presented, varying the Weissenberg number (Wi) and the spanwise wavenumber (β).

Figure 2 shows the neutral stability curves varying the Weissenberg number. The values considered were: $2, 6, 8, 10, 12$ and 14.

Figure 2 – Neutral Curve for the viscoelastic UCM model.

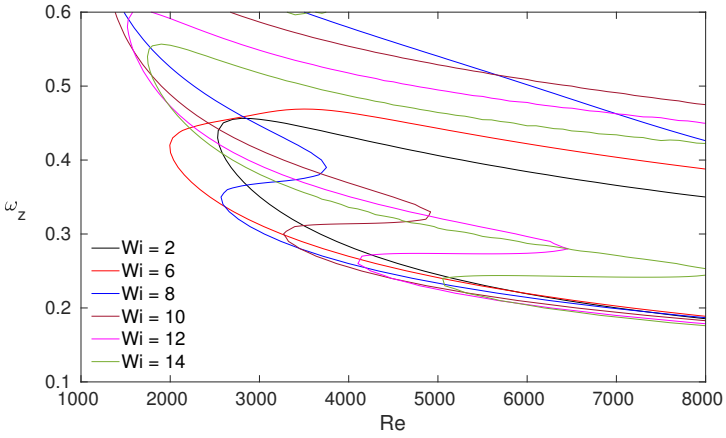

Source: Elaborated by the author.

It can be seen that the region where the amplification rates indicate wave growth (unsteady flow $\alpha_i < 0$) increases as the Weissenberg number is increased. The neutral curve that contains the largest unstable region is observed for $Wi = 8$, and then, with the increase of Wi to 10 and 12, this unstable region decreases consecutively. With the transition of values for the Weissenberg number from 6 to 8, it is possible to observe a significant change in the shape of the neutral curve. For both the values of $Wi = 2$ and 6, the neutral curve has the characteristic "banana" shape. However, when Wi is increased to 8, the neutral curve shape changes to a format where it seems to have two neutral curves with a banana shape, one overlapping the other, forming a "shark-like" design. This shark-like design is more pronounced when we look at the neutral curve obtained considering $Wi = 14$.

To explore this behaviour and look at how the three-dimensional disturbances behave for these values of the Weissenberg number, a variation of the three-dimensional wavenumber β was performed, considering: 0 (two-dimensional), $0.1, 0.2, 0.4, 0.6, 1.0$ and 1.2. Figures 3, 4 and 5 presents the neutral curves for three-dimensional disturbances considering $Wi = 8, 10$ and 12, respectively.

Increasing the value of the Weissenberg number from 6 to 8, it is evident that the instability region increases. Increasing the Weissenberg number value to 10, the instability region also increases, but it is possible to observe that the maximum frequency decreases. This behaviour becomes more evident when we look at Figure 5, where we can see that the maximum frequency decreases when the Weissenberg number increases to 12.

For the regions of instabilities considering neutral curves for three-dimensional disturbances, one can observe the validity of Squire's theorem. As the three-dimensional wavenumber β increases, the region of instability decreases. The three-dimensional wavenumber is a stabilising factor for models where Squire's theorem is satisfied.

Figure 3 – Neutral Curve for the viscoelastic UCM model for $Wi = 8$.

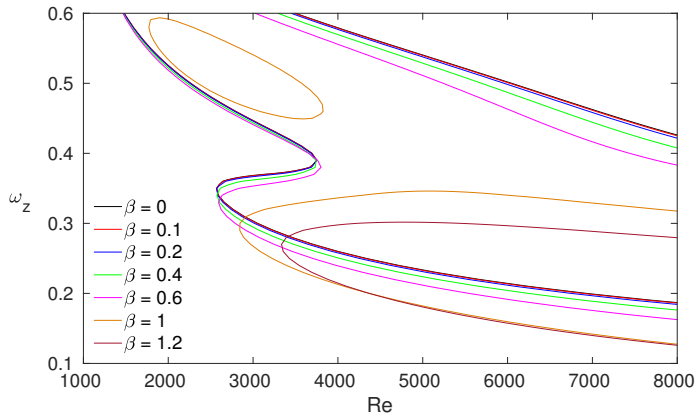

Source: Elaborated by the author.

Figure 4 – Neutral Curve for the viscoelastic UCM model for $Wi = 10$.

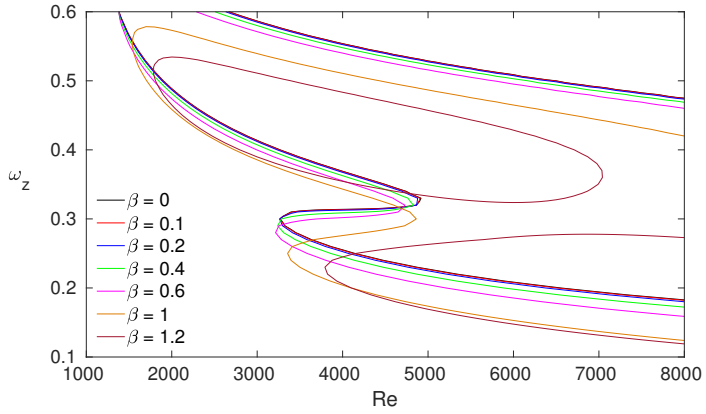

Source: Elaborated by the author.

An interesting behaviour can be observed in Figure 3. The neutral curve for $\beta = 1$ presents two separate instability regions. As the Weissenberg number increases, these regions merge. This behaviour repeats for the instability region for $\beta = 1.2$. For neutral curves considering Weissenberg 12, the regions of instabilities have no discontinuities. All regions for lower Weissenberg numbers were separated, merged and remains this way as the Weissenberg number value increased.

5.1.2 Oldroyd-B Results

Here, the results for stability analysis are presented, considering the Oldroyd-B model as the constitutive model for the viscoelastic fluid flow. Neutral stability curves are presented, varying the Weissenberg number (Wi) and the constant that controls the contribution of the solvent to the mixture (β_{nn}). Figures 6, 7 and 8 shows the neutral stability curves varying the Weissenberg number for different values for β_{nn}. The values considered for the Weissenberg

Figure 5 – Neutral Curve for the viscoelastic UCM model for $Wi = 12$.

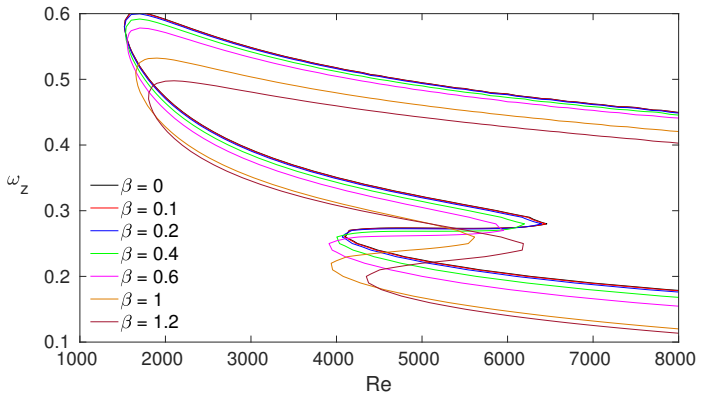

Source: Elaborated by the author.

number were: $2, 6, 8, 10, 12$ and 14 and for the constant β_{nn} were: $0.125, 0.5$ and 0.875.

Figure 6 – Neutral Curve for the viscoelastic Oldroyd-B model for $\beta_{nn} = 0.125$.

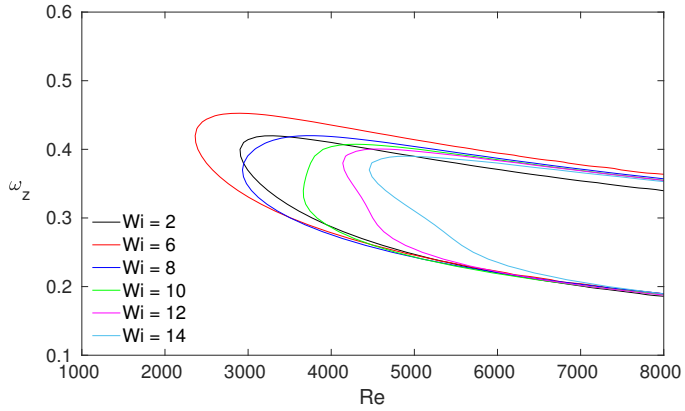

Source: Elaborated by the author.

The addition of solvent to the mixture has a stabilising effect on the flow. The instability region reduces considerably when we look at the difference in the neutral curves for the UCM and Oldroyd-B model. Moreover, for the graphs of the Oldroyd-B model, it is possible to see that this stabilising effect of the solvent addition continues to act. The instability region decreases considerably as the fluid mixture gains more Newtonian contribution in its composition (solvent addition).

Figure 6 shows the Weissenberg number (elasticity) effect on the instability region. As the value of this parameter increases from 2 to 6, the instability region increases. When this parameter reaches the value of 8, the instability region decreases again and continues for the other increased values. More solvent contribution in the mixture makes this behaviour disappears, showing that elasticity and polymer viscosity has a more significant effect on stability than solvent viscosity, whose destabilizing influence exists only for high Reynolds numbers.

Figure 7 – Neutral Curve for the viscoelastic Oldroyd-B model for $\beta_{nn} = 0.5$.

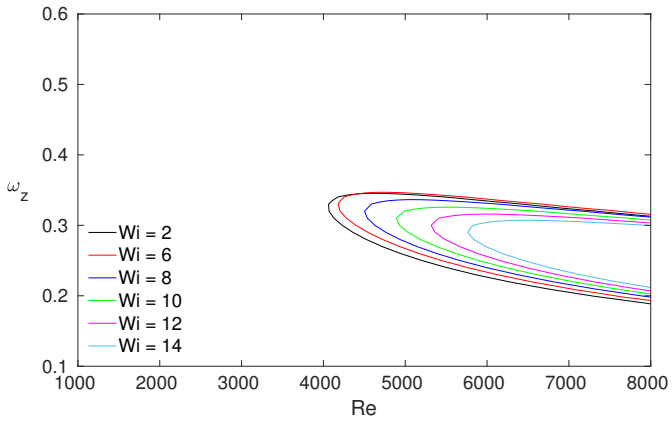

Source: Elaborated by the author.

Figure 8 – Neutral Curve for the viscoelastic Oldroyd-B model for $\beta_{nn} = 0.875$.

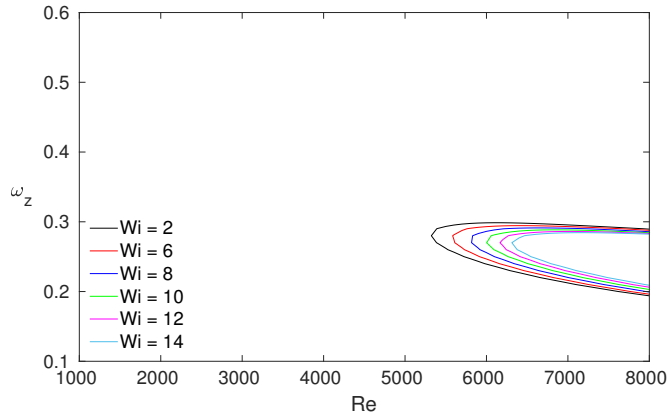

Source: Elaborated by the author.

As this viscoelastic model satisfies Squire's theorem and we do not notice any particular behaviour in the neutral curves considering three-dimensional disturbances, we present only two-dimensional ones, which are the most important for the stability analysis of this model.

5.2 Giesekus Model

This section presents the results obtained for stability analysis of the Giesekus viscoelastic model for two- and three-dimensional flows.

5.2.1 Two-Dimensional Disturbances Analysis

For the results' verification, Table 3 presents comparisons between the results presented by Blonce (1997) for stability analysis of two-dimensional flows for the Giesekus model with the results obtained using the method presented in this work.

This comparison is performed using the null α_i amplification rate (i.e., for values on the boundary of the neutral curve), obtained by solving the system (4.5).

Blonce (1997) uses different variables than the one used in this work, such as the parameter E, written as $E = \frac{Wi}{Re}$, and in the equations for the disturbances wave velocity c is used. To verify the results presented in this work, the value of $E = 8.6 \times 10^{-4}$ was adopted for the parameter E.

Table 3 – Comparison between the wavenumber presented in Blonce (1997) and the results obtained in this work.

β_{nn}	α_G	Re	Wi	ω	Blonce α_r	Pres. work α
0.2	0.1	5489.34	4.7208324	0.20714960	1.0420	$1.04479 - 0.0001852i$
	0.3	4064.09	3.4951174	0.22218604	1.0636	$1.06330 + 0.0000652i$
	0.5	3593.21	3.0901606	0.22995984	1.0776	$1.07750 + 0.0000814i$
0.5	0.1	4944.61	4.2523646	0.2368872	0.9970	$1.00125 - 0.0000443i$
	0.3	4271.79	3.6737394	0.24407986	1.0061	$1.00599 + 0.0000021i$
	0.5	4070.37	3.5005182	0.25105788	1.0107	$1.02064 - 0.0004362i$
0.8	0.1	5350.89	4.6017654	0.2592267	1.013	$1.01298 + 0.0000149i$
	0.3	5092.37	4.3794382	0.26411704	1.0174	$1.02031 - 0.0000313i$
	0.5	4980.98	4.2836428	0.26445452	1.0187	$1.01853 + 0.0000114i$

The results of the present work were performed using 150 Chebyshev modes.

The parameter α_G of the Giesekus model influences two- and three-dimensional disturbances. Therefore, it is necessary to analyse the influence of this parameter under both types of disturbances. For two-dimensional disturbances, a variation of this parameter was performed considering different values of β_{nn} and of the Weissenberg number to analyse its influence under many different conditions and flow characteristics.

Figure 9 presents the neutral stability curves for two-dimensional disturbances by varying the values of the parameter α_G, considering $Wi = 2$.

It is possible to observe that the parameter α_G, for these cases analysed, acts as a stabilising factor in the flow. In the graphs where the curves do not appear, the stabilisation was so high that the critical Reynolds is upper than 8000. As the percentage of solvent viscosity contribution increases in the fluid mixture ($\beta_{nn} \to 1$), this stabilising effect becomes smaller, to the point that the neutral curves for $\beta_{nn} = 0.75$ do not show many differences between the Oldroyd-B fluid ($\alpha_G = 0$) and the Giesekus fluid.

Another very expressive behaviour in these results is precisely how the neutral curve decreases in size (increasing the critical Reynolds) and then increases its size again (decreasing the critical Reynolds) as the values of the parameter α_G increase. This behaviour is more pronounced when we look at the neutral curves considering smaller values for β_{nn}, that is, the most significant non-Newtonian contribution in the fluid mixture (about 87.5%). As the Newtonian contribution increases in the fluid mixture, this behaviour reduces, as shown in Figure

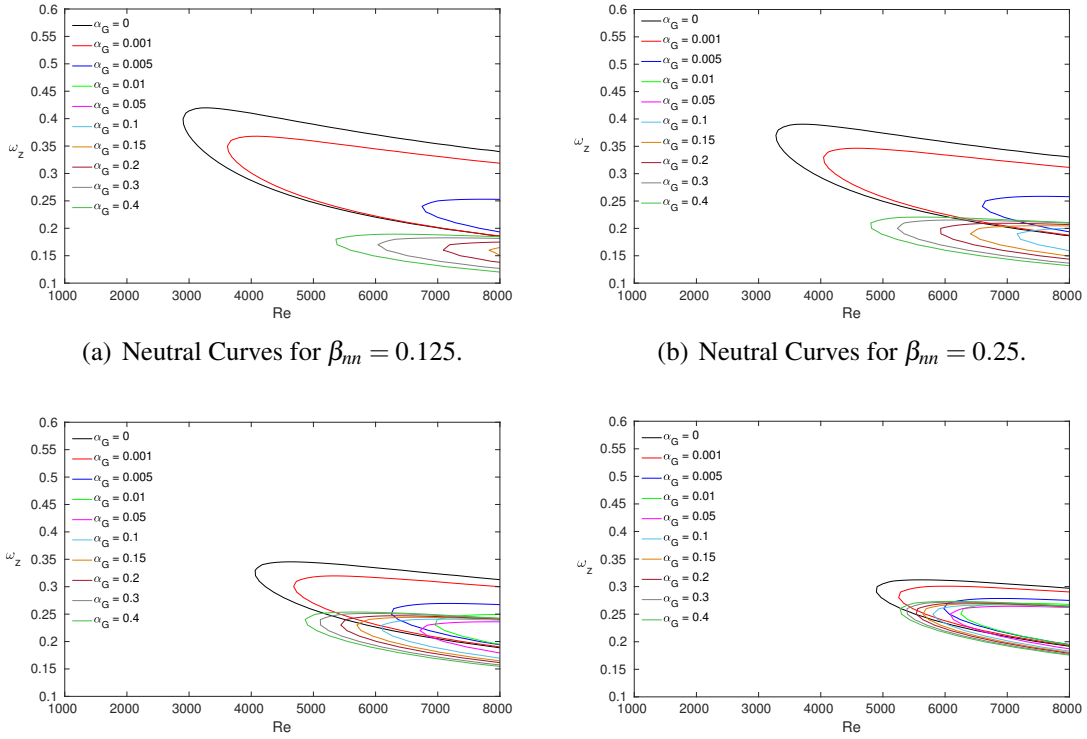

(a) Neutral Curves for $\beta_{nn} = 0.125$.

(b) Neutral Curves for $\beta_{nn} = 0.25$.

(c) Neutral Curves for $\beta_{nn} = 0.5$.

(d) Neutral Curves for $\beta_{nn} = 0.75$.

Figure 9 – Neutral curves for two-dimensional disturbances for different values of α_G considering $Wi = 2$.

9(d).

As this parameter is related to the mobility of the fluid, it is interesting to analyse its influence as the elasticity of the fluid increases. Figure 10 presents the neutral stability curves for two-dimensional disturbances by varying the values of the parameter α_G, considering $Wi = 6$.

The parameter α_G stabilising effect held for small values even with increasing Weissenberg. It can be observed that this effect was stronger, as a small increase in its value $0 \rightarrow 0.001$, caused the critical Reynolds to increase from ≈ 2500 to more than 8000 (considering the cases $\beta_{nn} = 0.125$ and 0.25). It is also possible to observe that, as the value of the parameter α_G increases (values greater than 0.05), the critical Reynolds decreases to the point that for $\alpha_G = 0.4$, the critical Reynolds is smaller than for the Oldroyd-B model.

When the value of the Weissenberg number increases to 8, we can observe the behaviour of the neutral stability curves in Figure 11.

The critical Reynolds value decreases as the Weissenberg number increases for higher amounts of polymer viscosity in the mixture. When the amount of solvent viscosity in the mixture increases, this behaviour is not as noticeable as the amount of polymer viscosity is high. However, the increase in the parameter α_G continues to cause the instability regions to increase after a particular value. The results show the influence of the parameter α_G, which for low values stabilises, even considering higher values for the Weissenberg number. However, for higher

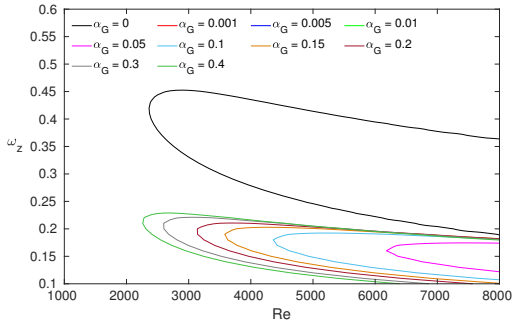

(a) Neutral Curves for $\beta_{nn} = 0.125$.

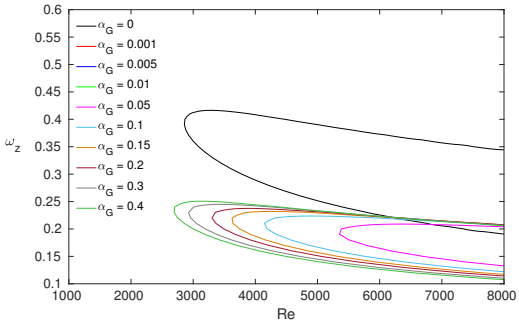

(b) Neutral Curves for $\beta_{nn} = 0.25$.

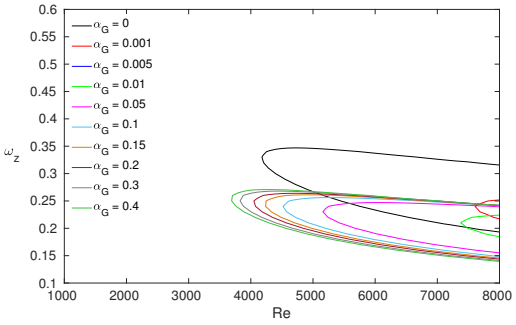

(c) Neutral Curves for $\beta_{nn} = 0.5$.

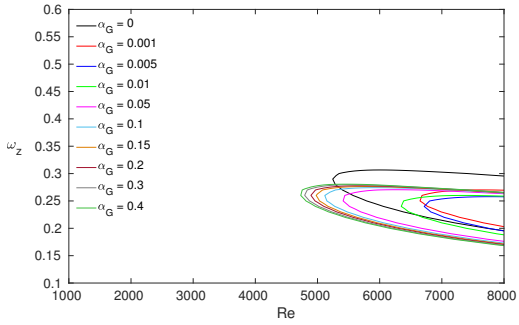

(d) Neutral Curves for $\beta_{nn} = 0.75$.

Figure 10 – Neutral curves for two-dimensional disturbances for different values of α_G considering $Wi = 6$.

values of this parameter, it is possible to observe that the destabilising effect also increases.

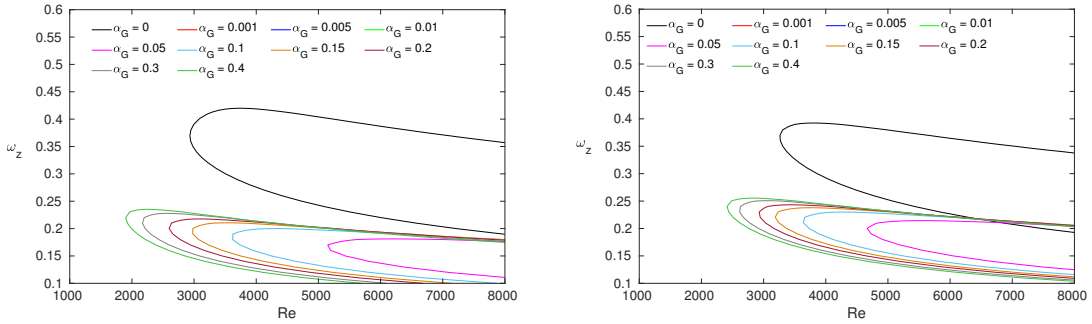

(a) Neutral Curves for $\beta_{nn} = 0.125$.

(b) Neutral Curves for $\beta_{nn} = 0.25$.

(c) Neutral Curves for $\beta_{nn} = 0.5$.

(d) Neutral Curves for $\beta_{nn} = 0.75$.

Figure 11 – Neutral curves for two-dimensional disturbances for different values of α_G considering $Wi = 8$.

The viscosity of the polymer has the effect of increasing the potential of the parameter α_G. For high amounts of polymer in the mixture, both the stabilising and destabilising effects have their potential increased, and as the amount of polymer decreases, both effects decrease their power.

Figure 12 presents the neutral curves for the same values of α_G considering $Wi = 10$.

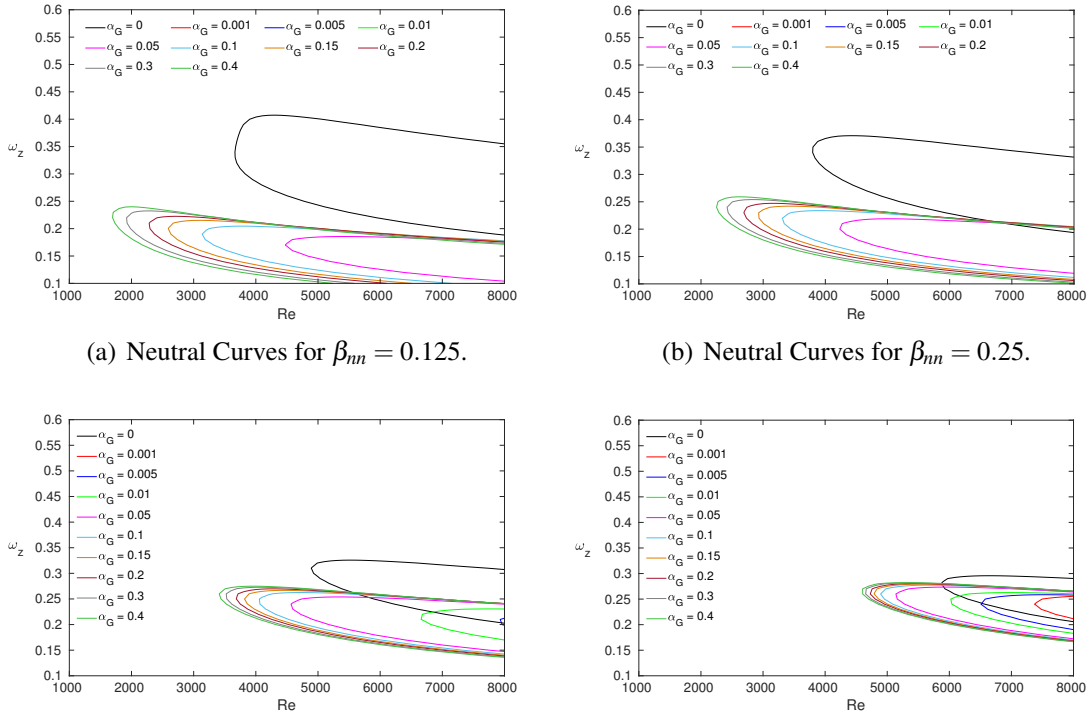

(a) Neutral Curves for $\beta_{nn} = 0.125$.

(b) Neutral Curves for $\beta_{nn} = 0.25$.

(c) Neutral Curves for $\beta_{nn} = 0.5$.

(d) Neutral Curves for $\beta_{nn} = 0.75$.

Figure 12 – Neutral curves for two-dimensional disturbances for different values of α_G considering $Wi = 10$.

Figure 12 shows that the behaviour exhibited by the influence of the parameter α_G holds for this value of the Weissenberg number.

5.2.2 Three-Dimensional Disturbances Analysis

Table 4 presents the comparison with the results obtained by Araujo (2021) with the results obtained by the LST technique considering three-dimensional disturbances in the flow of the viscoelastic fluid for the Giesekus model. Araujo (2021) solved the stability problem for this same viscoelastic model using the Direct Numerical Simulation (DNS) technique.

Table 4 shows a good agreement between the results obtained by the two computational techniques for stability analysis. This agreement assures the quality of the results obtained in this work considering three-dimensional disturbances.

As presented in Chapter 3, it is impossible to predict the behaviour of three-dimensional disturbances by considering Squire's theorem for the Giesekus model. Therefore, it is necessary

Table 4 – Comparison between the amplification rate obtained with the LST and DNS techniques.

β_{nn}	α_G	Re	Wi	ω	β	α_r	α_i - LST	α_i - DNS
0.25	0.005	12000	8	0.13	0	0.7855341	0.00418969	0.00426669
0.25	0.005	12000	8	0.13	0.8	0.6020718	−0.01026497	−0.01055978
0.50	0.1	3400	6	0.29	0.1	1.0996964	0.01029414	0.01042072
0.50	0.1	3400	6	0.29	0.8	0.9874944	0.02556869	0.02554535
0.50	0.15	7300	8	0.20	0.2	0.92538702	−0.01351977	−0.01349773
0.75	0.4	4700	8	0.27	1.2	0.82048732	0.06034785	0.06012240

The results of the present work were performed using 150 Chebyshev modes.

to perform an analysis solely for these disturbances.

An immediate consequence of this non-validity of Squire's theorem for a viscoelastic fluid is that for a given Reynolds value and frequency, the three-dimensional disturbances could be more unstable than the two-dimensional ones. This behaviour is illustrated in Figure 13. This Figure shows neutral stability curves for different values for the spanwise wavenumber β. These are: 0 (two-dimensional), $0.1, 0.2, 0.4, 0.6, 0.8, 1$ and 1.2.

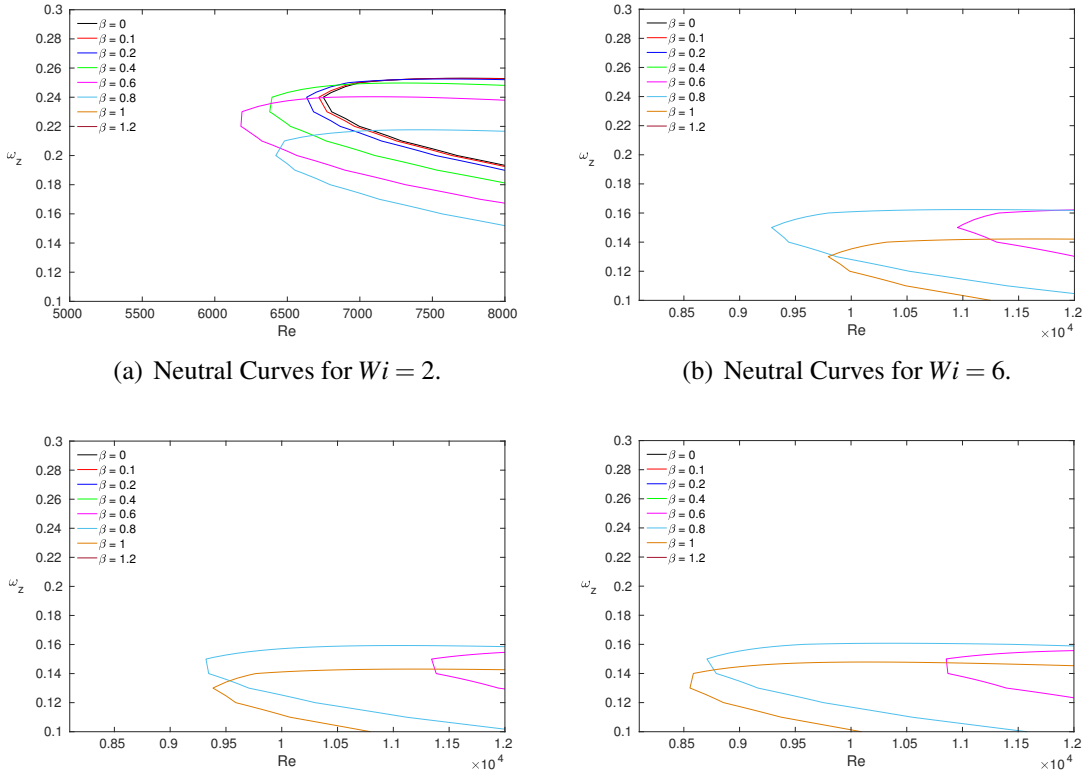

(a) Neutral Curves for $Wi = 2$.

(b) Neutral Curves for $Wi = 6$.

(c) Neutral Curves for $Wi = 8$.

(d) Neutral Curves for $Wi = 10$.

Figure 13 – Neutral curves for three-dimensional disturbances for different values of β considering $\beta_{nn} = 0.125$ and $\alpha_G = 0.005$.

Fig. 13 shows that, as verified in the graphs of the previous section, increasing the Weissenberg number stabilises two-dimensional disturbances. This effect is so strong that, from

$Wi = 6$, the critical Reynolds for these disturbances is above 12000. However, for $Wi = 2$, it is possible to observe the non-validity of Squire's theorem for this fluid. The increase of the spanwise wavenumber causes a reduction in the critical Reynolds value for the neutral curves of the three-dimensional disturbances. The increase of the spanwise wavenumber causes possible anticipation of the transition, characterising a destabilising factor for these flows. This behaviour is more pronounced as the Weissenberg number increases. The critical Reynolds for the two-dimensional disturbances of these flows are above 12000, but the smallest critical Reynolds for the three-dimensional disturbances of these flows are: ≈ 9285.937 for $Wi = 6$, ≈ 9320.41 for $Wi = 8$, and ≈ 8585.16 for $Wi = 10$.

Therefore, for fluid flows of this viscoelastic model, three-dimensional disturbances can be much more unstable than two-dimensional ones. For a better analysis of the effect of the spanwise wavenumber under the stability of the flows of this viscoelastic model, the two-dimensional cases presented in the section will be analysed by considering variations for β. These results are present in the form of the critical Reynolds numbers. To standardise and make it easier to understand the graphs, for the different values of the Giesekus model parameter α_G, the colours used for these two-dimensional curves in the previous section were kept.

Figure 14 presents the variation of the critical Reynolds values for different values of the Giesekus model parameter α_G, considering $Wi = 2$.

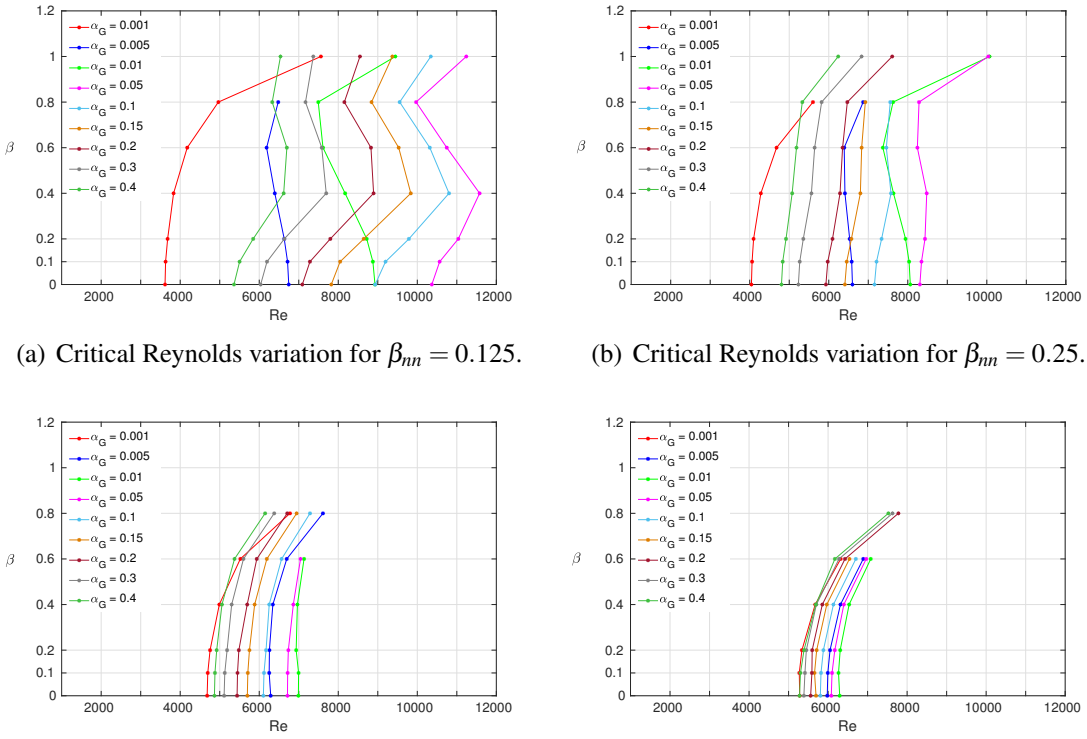

(a) Critical Reynolds variation for $\beta_{nn} = 0.125$.

(b) Critical Reynolds variation for $\beta_{nn} = 0.25$.

(c) Critical Reynolds variation for $\beta_{nn} = 0.5$.

(d) Critical Reynolds variation for $\beta_{nn} = 0.75$.

Figure 14 – Critical Reynolds number for three-dimensional disturbances for different values of β and α_G.

It is worth noting some flows do not have points for spanwise wavenumbers. It is because, for these wavenumbers, stabilisation has caused the critical Reynolds above 12000.

Fig. 14 shows that as the Newtonian contribution in the fluid mixture increases, the range of values for critical Reynolds decreases, pronouncing the influence of the polymer viscosity on the stability of the flows.

The anisotropic effect that is inserted in this model through the term accompanying the parameter α_G in the constitutive equation suffers influence both on the polymer viscosity (this term is divided by $(1-\beta_{nn})$) and on the elasticity (as this term is multiplied by Wi) as observed in Figure 14, the polymer viscosity exhibit a significant influence on the behaviour that characterises the non-validity of Squire's theorem.

To analyze the influence of elasticity under the three-dimensional disturbances and its stabilizing/destabilizing factor, Figures 15, 16 and 17 present the variation of Reynolds number values considering Weissenberg number $6, 8$ and 10 respectively.

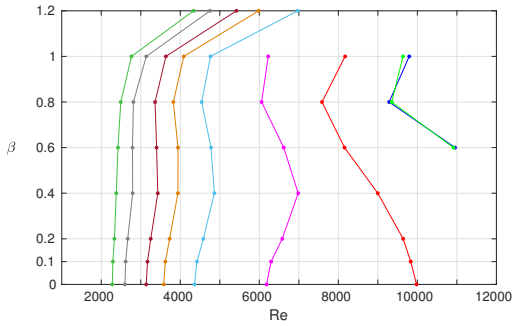

(a) Critical Reynolds variation for $\beta_{nn} = 0.125$.

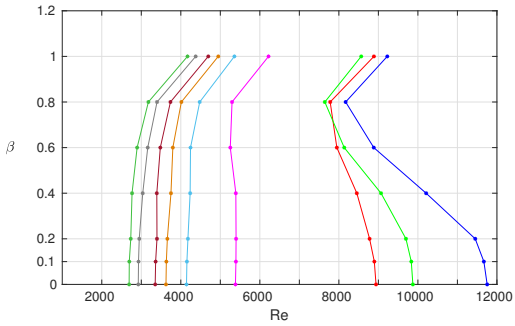

(b) Critical Reynolds variation for $\beta_{nn} = 0.25$.

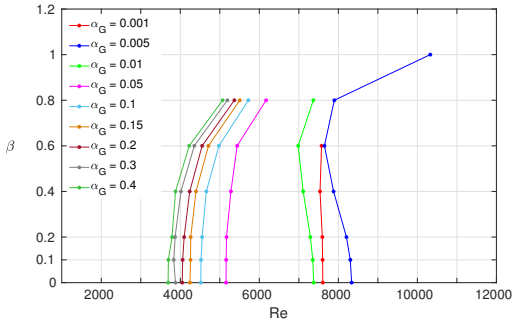

(c) Critical Reynolds variation for $\beta_{nn} = 0.5$.

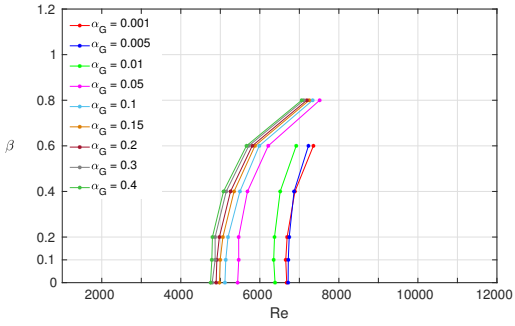

(d) Critical Reynolds variation for $\beta_{nn} = 0.75$.

Figure 15 – Critical Reynolds number for three-dimensional disturbances for different values of β and α_G for $Wi = 6$.

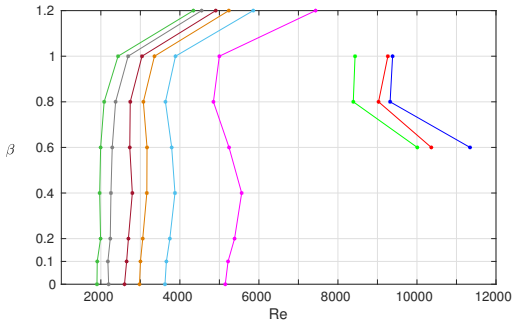

(a) Critical Reynolds variation for $\beta_{nn} = 0.125$.

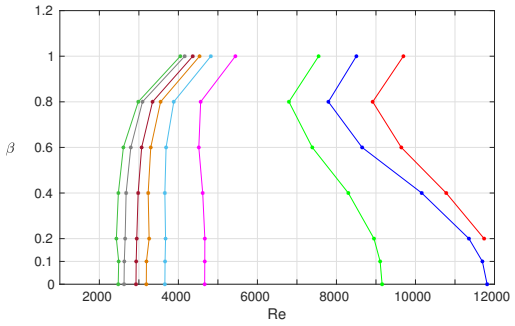

(b) Critical Reynolds variation for $\beta_{nn} = 0.25$.

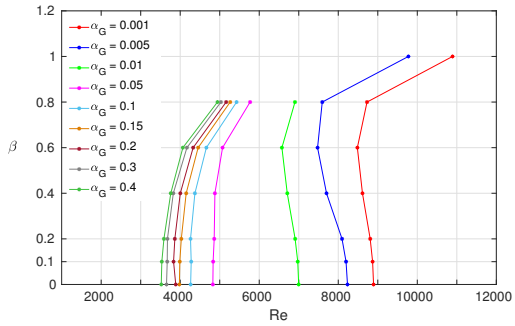

(c) Critical Reynolds variation for $\beta_{nn} = 0.5$.

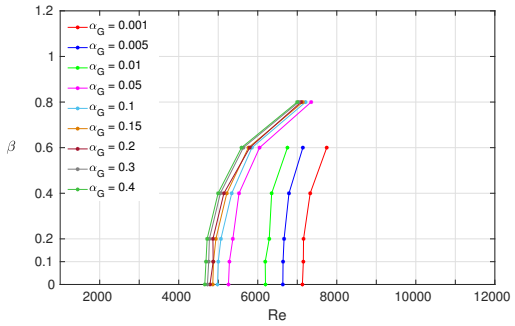

(d) Critical Reynolds variation for $\beta_{nn} = 0.75$.

Figure 16 – Critical Reynolds number for three-dimensional disturbances for different values of β and α_G $Wi = 8$.

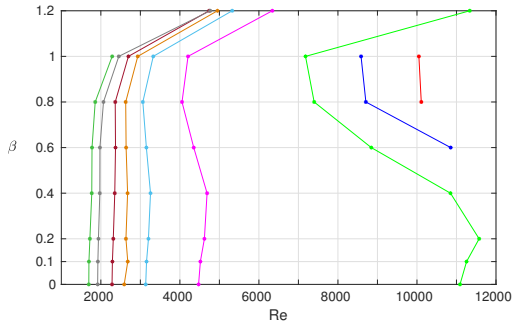

(a) Critical Reynolds variation for $\beta_{nn} = 0.125$.

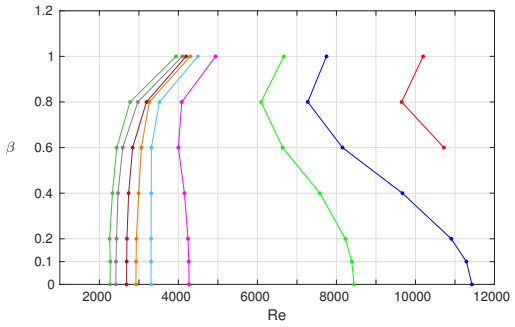

(b) Critical Reynolds variation for $\beta_{nn} = 0.25$.

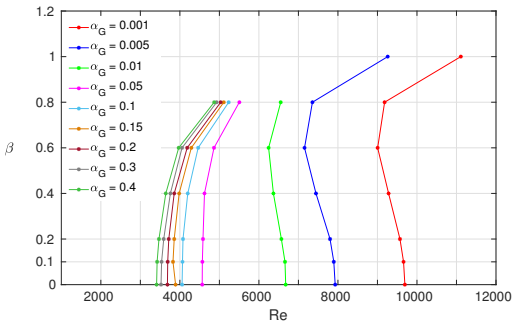

(c) Critical Reynolds variation for $\beta_{nn} = 0.5$.

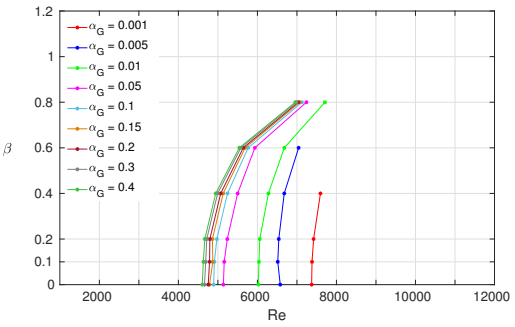

(d) Critical Reynolds variation for $\beta_{nn} = 0.75$.

Figure 17 – Critical Reynolds number for three-dimensional disturbances for different values of β and α_G $Wi = 10$.

It becomes evident that for the Giesekus model, low values of parameter α_G increase the anisotropic effect under the three-dimensional disturbances. This statement is evident because this term is responsible for the non-validity of Squire's theorem. As the value for this parameter increases, the spanwise wavenumber becomes a stabilising factor or at least reduces its destabilising effect. Increasing the value of the parameter α_G makes two-dimensional disturbances the most dangerous for the flow transition. As the Newtonian contribution increases, a reduction in the effect of the non-validity of Squire's theorem is observed. In the constitutive equation, the increase in the value of β_{nn} implies a larger contribution of the term accompanying the parameter α_G (since $(1-\beta_{nn}) \to 0$).

As the Weissenberg number increases, three-dimensional disturbances become more predominant in the flow's destabilization. Even with the solvent contribution increase, which has the characteristic of stabilization, it is possible to observe a reduction of the critical Reynolds value for $\beta_{nn} = 0.5$, showing that the three-dimensional disturbances remain more unstable than the two-dimensional ones. This shows the influence of the effect of elasticity on flow stability. Higher elasticity in the viscoelastic fluid means a major influence of three-dimensional disturbances on flow stability. If combined with low values for the parameter α_G and with high polymer viscosity in the mixture, one can have a reduction in the critical Reynolds value from ≈ 11000 for two-dimensional disturbances to ≈ 7000 considering $\beta = 1$ (Fig. 17(a)) for the same flow.

5.3 LPTT model

This section presents a few results obtained for stability analysis of the LPTT viscoelastic model for two- and three-dimensional flows.

For the analysis of the two-dimensional disturbances, the neutral curves were performed, considering variations for the parameter ξ and the Weissenberg number. The values considered for the results were $\beta_{nn} = 0.25$ and 0.50. The parameter $\varepsilon = 0.75$, the values of ξ were $0.01, 0.05, 0.1, 0.15$ and 0.2. The values for the Weissenberg number were $2, 6$ and 8.

Figure 18 presents the neutral stability curves for two-dimensional disturbances.

It can be seen that as the Weissenberg number increases, the increase in the parameter ξ causes an increase in the instability region (reduction of the critical Reynolds). To understand how the polymer viscosity influences the flow stability of the LPTT model, Figure 19 presents the neutral stability curves considering $\beta_{nn} = 0.25$.

For a higher amount of polymer viscosity in the fluid mixture, the parameter ξ exhibit a stabilizing effect when considering $Wi = 2$.

The same analysis done for the Giesekus fluid flows was performed for the LPTT model flows for the three-dimensional disturbances. The flows for two-dimensional disturbances were

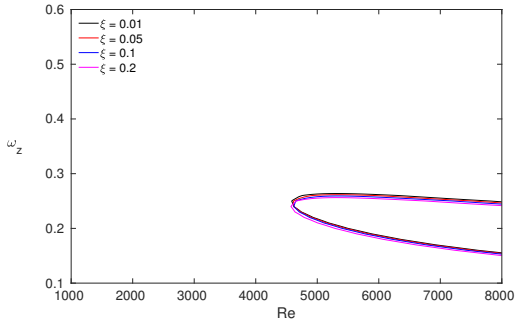

(a) Neutral Curves for $Wi = 2$.

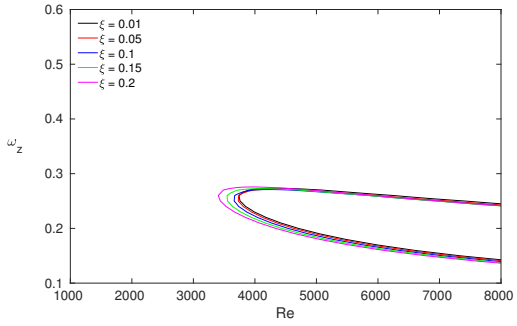

(b) Neutral Curves for $Wi = 6$.

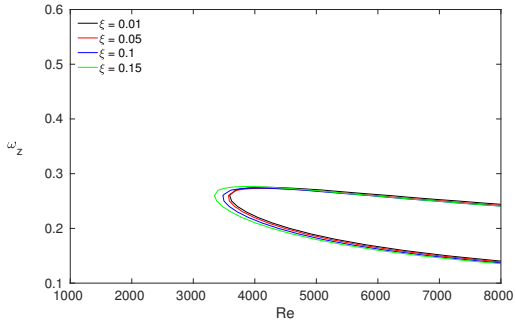

(c) Neutral Curves for $Wi = 8$.

Figure 18 – Neutral curves for two-dimensional disturbances for different values of ξ considering $\beta_{nn} = 0.50$ and $\varepsilon = 0.75$.

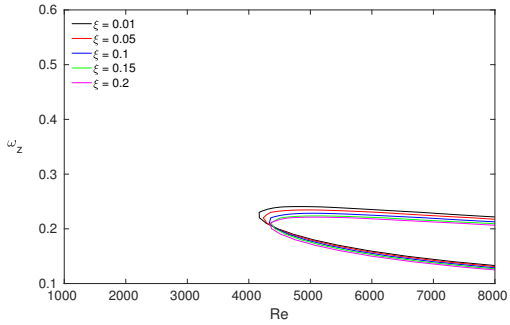

Figure 19 – Neutral curves for two-dimensional disturbances for different values of ξ considering $\beta_{nn} = 0.25, \varepsilon = 0.75$ and $Wi = 2$.

performed considering different values for the spanwise wavenumber β. For this, the values of β were varied in the form $0(two-dimensional), 0.1, 0.2, 0.4, 0.6, 0.8, 1$ and 1.2.

For the cases performed considering the viscoelastic LPTT model, it was impossible to verify the non-validity of Squire's theorem as in the Giesekus model. A more thorough investigation needs to be performed, varying the values for the parameter ε, which is responsible for the non-validity of the theorem for this model.

Figure 21 presents the variation of the values for the critical Reynolds number considering the flows presented in Fig. 19.

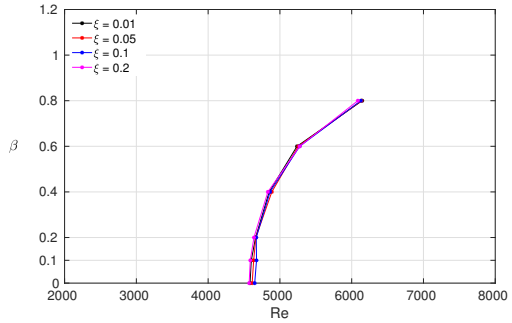

(a) Critical Reynolds variation for $Wi = 2$.

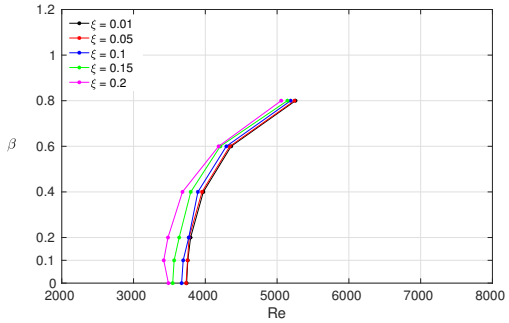

(b) Critical Reynolds variation for $Wi = 6$.

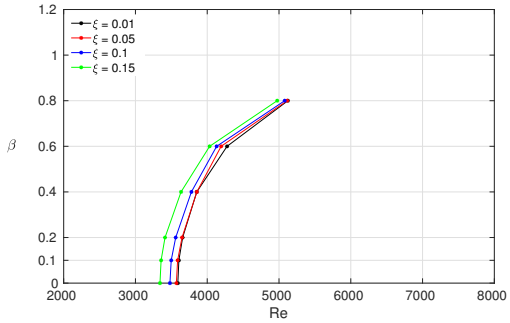

(c) Critical Reynolds variation for $Wi = 8$.

Figure 20 – Critical Reynolds number for three-dimensional disturbances for different values of β and ξ.

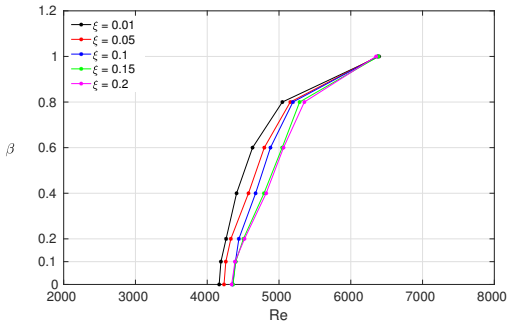

Figure 21 – Critical Reynolds number for three-dimensional disturbances for different values of β and ξ.

As in the previous Figure, verifying the non-validity of Squire's theorem is impossible considering three-dimensional disturbances.

CHAPTER

6

CONCLUSIONS AND FUTURE WORK

This work presents the stability analysis for viscoelastic fluid flows, governed by the constitutive equation called here LPOG (2.9), which contains four viscoelastic models, Upper-Convected Maxwell (UCM), Oldroyd-B, Giesekus and LPTT.

Linear Stability Theory was adopted to investigate the stability of viscoelastic fluid flows to non-stationary disturbances, particularly the three-dimensional, incompressible, isothermal viscoelastic flow between parallel plates. It is worth noting that, in the present work, only the spatial analysis of the propagation of disturbances was performed by constructing the neutral stability curves.

A study was carried out on the validity of Squire's theorem for viscoelastic fluid models. This study shows the relationship of the validity of Squire's theorem with the isotropy of the model considered. Viscoelastic models that present anisotropy in their rheological properties cause the failure of the validity of Squire's theorem. This theorem is based on the projection of the fluid properties onto the wave propagation directions. Anisotropy does not allow these projections to be made, indicating that the rheological properties of these fluids vary differently depending on the direction considered.

The results of the UCM and Oldroyd-B models confirmed what was already known in the literature. The validity of Squire's theorem for these models helped verify the results considering three-dimensional disturbances. An unusual behaviour was verified for the UCM model when considering higher values for the Weissenberg number. This model presents a change in the shape of the stability regions, commonly known as banana-shape, these regions increase considerably in size, and their shape becomes similar to a shark shape.

The results for the Giesekus model considering two-dimensional disturbances were validated using results presented in the literature by Blonce (1997). The results presented by this author consider only values on top of the neutral stability curve (i.e., $\alpha_i = 0$), and the results obtained using the formulation presented in this work showed an excellent agreement, presenting

a difference of 10^{-4} in the values. The results for this model considering three-dimensional disturbances were verified using the results presented by Araujo (2021). The results obtained for the Giesekus model show the influence of the parameter of this model α_G under the stability of the flows. For two-dimensional disturbances, it could be verified that small values for this parameter bring stability to the flow, increasing the value of the critical Reynolds. However, as this parameter increases, the opposite effect is verified, becoming a destabilizing factor in the flow. These characteristics are intensified with the increase of the Weissenberg number and when considering higher polymer viscosity in the fluid mixture. For three-dimensional disturbances, it could be verified that the effect of the non-validity of Squire's theorem (three-dimensional disturbances presenting lower critical Reynolds than the two-dimensional ones) is more intense when considering lower values for the parameter α_G, as well as high contribution of the polymer viscosity in the mixture and also higher values for the Weissenberg number.

The stability analysis results for the LPTT model were not verified as exciting and expressive behaviours as for the Giesekus model. Therefore a continuation of the investigations regarding the stability of this fluid is necessary.

As a continuation of this research, the proposal is to analyze more cases where the characteristic behaviours and the stability of each viscoelastic model are remarkable, including the more significant variation of the parameters to understand better their effects on the stabilization and destabilization of these flows. Also, the energy analysis of the perturbations is a work for the future, being able to say which terms contribute to amplifying or smoothing the disturbances analyzed.

BIBLIOGRAPHY

ALVES, M.; PINHO, F.; OLIVEIRA, P. Study of steady pipe and channel flows of a single-mode Phan-Thien-Tanner fluid. **Journal of Non-Newtonian Fluid Mechanics**, v. 101, p. 55–76, 2001. Citation on page 50.

ARAUJO, M. T. **Estudo de Escoamentos Transicionais Tridimensionais de Fluidos Viscoelásticos modelados por Giesekus**. Phd Thesis (PhD Thesis) — Universidade de São Paulo, 2021. Citations on pages 64 and 74.

ARAUJO, M. T.; FURLAN, L. J. S.; BRANDI, A. C.; SOUZA, L. F. A semi-analytical method for channel and pipe flows for the linear phan-thien-tanner fluid model with a solvent contribution. **Polymers**, v. 14, n. 21, 2022. ISSN 2073-4360. Available: <https://www.mdpi.com/2073-4360/14/21/4675>. Citation on page 50.

AVGOUSTI, M.; BERIS, A. N. Non-axisymmetric modes in viscoelastic Taylor-Couette flow. **Journal of Non-Newtonian Fluid Mechanics**, v. 50, n. 2, p. 225 – 251, 1993. Citation on page 27.

BERIS, A.; ARMOSTRONG, R.; BROWN, R. Spectral finite-element calculations of the flow of a Maxwell fluid between excetric rotating cylinders. **Journal of Non-Newtonian Fluid Mechanics**, v. 22, p. 129–167, 1987. Citations on pages 25 and 30.

BIRD, R. B.; ARMSTRONG, R. C.; HASSAGER, O. **Dynamics of polymeric liquids**. [S.l.]: John Willey & Sons, 1987. Citations on pages 26 and 30.

BIRD, R. B.; DEAGUIAR, J. R. An encapsulated dumbbel model for concentrated polymer solutions and melts i. theoretical development and constitutive equation. **Journal of Non-Newtonian Fluid Mechanics**, v. 13, p. 149–360, 1983. Citation on page 26.

BIRD, R. B.; DOTSON, P. J.; JOHNSON, N. L. Polymer solution rheology based on a finitely extensible bead-spring chain model. **Journal of Non-Newtonian Fluid Mechanics**, v. 7, p. 213–235, 1980. Citation on page 26.

BISTAGNINO, A.; BOFFETTA, G.; CELANI, A.; MAZZINO, A.; PULIAFITO, A.; VERGASSOLA, M. Nonlinear dynamics of the viscoelastic Kolmogorov flow. **Journal of Fluid Mechanics**, Cambridge University Press, v. 590, p. 61–80, 2007. Citation on page 40.

BLONCE, L. Linear stability of Giesekus fluid in Poiseuille flow. **Mechanics Research Communications**, v. 24, n. 2, p. 223–228, 1997. ISSN 0093-6413. Available: <https://www.sciencedirect.com/science/article/pii/S0093641397000165>. Citations on pages 17, 27, 46, 59, 60, and 73.

BRANDI, A. C.; MENDONçA, M. T.; SOUZA, L. F. Dns and lst stability analysis of Oldroyd-B fluid in a flow between two parallel plates. **Journal of Non-Newtonian Fluid Mechanics**, v. 267, p. 14 – 27, 2019. Citations on pages 27, 49, and 53.

BRASSEUR, E.; FYRILLAS, M.; GEORGIOOU, G.; CROCHET, M. The time-dependent extrudate-swell problem of an Oldroyd-B fluid with slip along the wall. **Journal of Rheology**, v. 42, p. 549–566, 1994. Citations on pages 25 and 30.

CASTILLO, H. A.; WILSON, H. J. Towards a mechanism for instability in channel flow of highly shear-thinning viscoelastic fluids. **Journal of Non-Newtonian Fluid Mechanics**, v. 247, p. 15–21, 2017. ISSN 0377-0257. Available: <https://www.sciencedirect.com/science/article/pii/S0377025717301532>. Citations on pages 27 and 45.

CHRISTIANSEN, R. L.; BIRD, R. B. Dilute solution rheology: experimental results and finitely extensible nonlinear elastic dumbbell theory. **Journal of Non-Newtonian Fluid Mechanics**, v. 3, p. 161–177, 1977. Citation on page 26.

DON, W. S.; SOLOMONOFF, A. Accuracy and speed in computing the Chebyshev collocation derivative. **SIAM Journal on Scientific Computing**, v. 16, p. 1253–1268, 1995. Citation on page 51.

DRAAD, A. A.; KUIKEN, G. D. C.; NIEUWSTADT, F. T. M. Laminar–turbulent transition in pipe flow for newtonian and non-newtonian fluids. **Journal of Fluid Mechanics**, Cambridge University Press, v. 377, p. 267–312, 1998. Citation on page 27.

FURLAN, L. J. da S.; ARAUJO, M. T. de; BRANDI, A. C.; CRUZ, D. O. de A.; SOUZA, L. F. de. Different formulations to solve the Giesekus model for flow between two parallel plates. **Applied Sciences**, v. 11, n. 21, 2021. ISSN 2076-3417. Available: <https://www.mdpi.com/2076-3417/11/21/10115>. Citation on page 50.

FURLAN, L. J. S. **Análise de Estabilidade de Escoamentos do Fluido Viscoelástico Giesekus**. Master's Thesis (Master's Thesis) — Universidade Estadual Paulista "Julio de Mesquita Filho", 2018. Citation on page 27.

FURLAN, L. J. S.; MENDONCA, M. T.; ARAUJO, M. T.; SOUZA, L. F. On the validity of Squire's theorem for viscoelastic fluid flows. **Journal of Non-Newtonian Fluid Mechanics**, v. 307, p. 104880, 2022. ISSN 0377-0257. Available: <https://www.sciencedirect.com/science/article/pii/S0377025722001070>. Citation on page 47.

GERVAZONI, E. S. **Análise de estabilidade linear de escoamentos bidimensionais do fluido Oldroyd-B**. Master's Thesis (Master's Thesis) — Universidade Estadual Paulista "Júlio de Mesquita Filho", 2016. Citation on page 27.

GIESEKUS, H. Elasto-viskose flüssigkeiten, für die in stationären schichtströmungen sämtliche normalspannungskomponenten verschieden gross sind. **Rheologica Acta**, v. 2, p. 50–62, 1962. Citation on page 26.

____. A simple constitutive equation for polymer fluids based on the concept of deformation-dependent tensorial mobility. **Journal of Non-Newtonian Fluid Mechanics**, v. 11, p. 69–109, 1982. Citations on pages 26 and 30.

____. Constitutive equations for polymer fluids based on the concept of configuration-dependent molecular mobility: a generalized mean-configuration model. **Journal of Non-Newtonian Fluid Mechanics**, v. 17, n. 3, p. 349–372, 1985. ISSN 0377-0257. Available: <https://www.sciencedirect.com/science/article/pii/0377025785800264>. Citation on page 26.

KAYE, A. **Non-newtonian flow in incompressible flows**. [S.l.]: College of Aeronautics, 1962. Citation on page 26.

LARSON, R. G. **Constitutive equations for polymer melts and solutions**. [S.l.]: Butterworths, 1988. Citation on page 26.

____. Instabilities in viscoelastic flows. **Rheologica Acta**, v. 31, p. 213–263, 1992. Citation on page 27.

LARSON, R. G.; SHAQFEH, E. S. G.; MULLER, S. J. A purely elastic instability in Taylor-Couette flow. **Journal of Fluid Mechanics**, v. 218, p. 573–600, 1990. Citation on page 27.

LEE, K.-C.; FINLAYSON, B. A. Stability of plane poiseuille and couette flow of a maxwell fluid. **Journal of Non-Newtonian Fluid Mechanics**, v. 21, n. 1, p. 65–78, 1986. ISSN 0377-0257. Available: <https://www.sciencedirect.com/science/article/pii/0377025786800635>. Citation on page 27.

LEONOV, A. I. Nonequilibrium thermodynamics and rheology of viscoelastic polymer media. **Rheologica Acta**, v. 15, p. 85–98, 1976. Citation on page 26.

LIM, F.; SCHOWALTER, W. Pseudo-spectral analysis of the stability of pressure-driven flow of a giesekus fluid between parallel planes. **Journal of Non-Newtonian Fluid Mechanics**, v. 26, n. 1, p. 135–142, 1987. ISSN 0377-0257. Available: <https://www.sciencedirect.com/science/article/pii/0377025787850516>. Citation on page 27.

LUO, X. L.; TANNER, R. I. A streamline element scheme for solving viscoelastic flow problems part ii: Integral constitutive models. **Journal of Non-Newtonian Fluid Mechanics**, v. 22, p. 61–89, 1986. Citation on page 26.

____. Finite element simulation of long and short circlar die extrusion experiments using integral models. **International Journal for Numerical Methods in Engineering**, v. 25, p. 9–22, 1988. Citation on page 26.

MAK, J. **Hydrodynamic Stability of Newtonian and Non-Newtonian Fluids**. Phd Thesis (PhD Thesis) — University of Durham, 2009. Citation on page 27.

MARXEN, O. **Numerical studies of physical effects related to the controlled transition process in laminar separation bubbles**. Phd Thesis (PhD Thesis) — Institut für Aerodynamik und Gasdynamik der Universität Stuttgart, 2005. Citation on page 27.

MENDONÇA, M. T.; MEDEIROS, M. A. F. de. **Instabilidade Hidrodinâmica e transição para turbulência com aplicações em engenharia e meteorologia**. [S.l.]: ENCIT - 2002, 2002. Citation on page 28.

MOMPEAN, G.; DEVILLE, M. Unsteady finite volume of Oldroyd-B fluid through a three-dimensional planar contraction. **Journal of Non-Newtonian Fluid Mechanics**, v. 72, p. 253–279, 1997. Citation on page 25.

OLIVEIRA, P. J. An exact solution for tube and slit flow of a fene-p fluid. **Acta Mechanica**, v. 158, p. 157–167. ISSN 1619-6937. Citation on page 26.

PHAN-THIEN, N.; TANNER, R. I. A new constitutive equation derived from network theory. **Journal of Non-Newtonian Fluid Mechanics**, v. 2, p. 353–365, 1977. Citations on pages 26 and 30.

PHILLIPS, T. N.; WILLIAMS, A. Comparison of creeping and inertial flow of an oldroyd-b fluid though a planar and axisymmetric contraction. **Journal of Non-Newtonian Fluid Mechanics**, v. 108, p. 25–47, 2002. Citation on page 25.

PINHO, F. T.; ALVES, M. A.; OLIVEIRA, P. J. Benchmark solutions for the flow of Oldroyd-B and PTT fluids in planar contractions. **Journal of Non-Newtonian Fluid Mechanics**, v. 10, p. 45–75, 2003. Citations on pages 25 and 26.

PINHO, F. T.; OLIVEIRA, P. J. Axial annular flow of a nonlinear viscoelastic fluid — an analytical solution. **Journal of Non-Newtonian Fluid Mechanics**, v. 93, n. 2, p. 325–337, 2000. ISSN 0377-0257. Available: <https://www.sciencedirect.com/science/article/pii/S0377025700001130>. Citation on page 30.

RAJAGOPALAN, D.; ARMSTRONG, R. C.; BROWN, R. A. Finite element methdos for calculation of steady, viscoelastic flow using constitutive equations with a newtonian viscosity. **Journal of Non-Newtonian Fluid Mechanics**, v. 36, p. 159–192, 1990. ISSN 0377-0257. Available: <https://www.sciencedirect.com/science/article/pii/037702579085008M>. Citation on page 29.

RAM, A.; TAMIR, A. Structural turbulence in polymer solutions. **Journal of Applied Polymer Science**, v. 8, n. 6, p. 2751–2762, 1964. Available: <https://onlinelibrary.wiley.com/doi/abs/10.1002/app.1964.070080621>. Citation on page 27.

SAMANTA, D.; DUBIEF, Y.; HOLZNER, M.; SCHäFER, C.; MOROZOV, A. N.; WAGNER, C.; HOF, B. Elasto-inertial turbulence. **Proceedings of the National Academy of Sciences**, v. 110, n. 26, p. 10557–10562, 2013. Available: <https://www.pnas.org/doi/abs/10.1073/pnas.1219666110>. Citation on page 27.

SCHMID, P. J.; HENNINGSON, D. S. **Stability and Transition in Shear Flows**. [S.l.]: Springer, 2001. Citation on page 26.

SHAQFEH, E. S. G.; MULLER, S. J.; LARSON, R. G. The effects of gap width and dilute solution properties on the viscoelastic Taylor-Couette instability. **Journal of Fluid Mechanics**, v. 235, p. 285–317, 1992. Citation on page 27.

SILVA, A. A. **Simulação numérica da estabilidade de Escoamentos de um fluido Giesekus**. Master's Thesis (Master's Thesis) — Universidade de São Paulo, 2018. Citation on page 27.

SOUZA, L. F.; BRANDI, A. C.; MENDONçA, M. T. Estabilidade de escoamentos de fluidos não-Newtonianos. In: ____. 1. ed. [S.l.]: In: Turbulência, 2016. v. 10, p. 101–160. Citation on page 27.

SOUZA, L. F.; MENDONÇA, M. T.; MEDEIROS, M. A. F. The advantages of using high-order finite differences schemes in laminar-turbulent transition studies. **International Journal for Numerical Methods in Fluids**, v. 48, p. 565–592, 2005. Citation on page 26.

SQUIRE, H. B. On the Stability for Three-Dimensional Disturbances of Viscous Fluid Flow between Parallel Walls. **Proceedings of the Royal Society A**, v. 142, p. 621–628, 1933. ISSN 0950-1207. Available: <https://royalsocietypublishing.org/doi/abs/10.1098/rspa.1933.0193>. Citations on pages 28, 37, and 38.

STEVENSON, J. F.; BIRD, R. B. Elongational viscosity of nonlinear elastic dumbell suspensions. **Transactions of the Society of Rheology**, v. 15, p. 135–145, 1971. Citation on page 26.

SURESHKUMAR, R.; BERIS, A. N. Linear stability analysis of viscoelastic Poiseuille flow using an Arnoldi-based orthogonalization algorithm. **Journal of Non-Newtonian Fluid Mechanics**, v. 56, p. 151–182, 1995. Citation on page 27.

TANNER, R. I. **Engineering Rheology**. [S.l.]: Clarendon Press, 1988. Citation on page 29.

WARNER, H. R. Kinetic theory and rheology of dilute suspensions of finitely extendible dumbbells. **Industrial Engineering Chemistry Fundamentals**, v. 11, p. 379–387, 1972. Citation on page 26.

WEIDEMAN, J. A.; REDDY, S. C. A matlab differentiation matrix suite. **ACM Trans. Math. Softw.**, Association for Computing Machinery, New York, NY, USA, v. 26, n. 4, p. 465–519, dec 2000. ISSN 0098-3500. Available: <https://doi.org/10.1145/365723.365727>. Citation on page 51.

WHITE, J. L.; METZNER, A. B. Development of constitutive equations for polymeric melts and solutions. **Journal of Applied Polymer Science**, v. 7, p. 1867–1889, 1963. Citation on page 26.

ZHANG, M.; LASHGARI, I.; ZAKI, T. A.; BRANDT, L. Linear stability analysis of channel flow of viscoelastic Oldroyd-B and FENE-P fluids. **Journal of Fluid Mechanics**, v. 737, p. 249–279, 2013. Citation on page 27.

APPENDIX

A

ALGEBRAIC MANIPULATIONS IN THE SYSTEM OF EQUATIONS FOR THE MATRIX METHOD

The matrix method consists of rewriting the system of equations (2.24) - (2.33) in the form

$$LV = \alpha FV, \tag{A.1}$$

with the eigenvector, V is defined as

$$V = [u,\ \alpha u,\ v,\ \alpha v,\ w,\ \alpha w,\ p,\ T_{xx},\ T_{xy},\ T_{xz},\ T_{yy},\ T_{yz},\ T_{zz}]^T. \tag{A.2}$$

Here, the details of the mathematical manipulation required for this rewrite are presented.

The matrix system is therefore rewritten in such a way that each row of the matrix corresponds to an equation of the system (2.24) - (2.33), and the addition of 3 rows are required to make the system closed and the matrices square. The matrices L and F have the coefficients for the disturbances in the eigenvector V.

Defining the matrix L (left-hand side of the matrix equation (A.1)) and the matrix F (right-hand side of the matrix equation Eq. (A.1)) in the form with the subindexes (i, j) of $L_{i,j}$ and $F_{i,j}$ denote row and column, respectively.

For consistency and familiarity with the subindex notation, we rewrite the eigenvector (A.2) as follows:

$$V = [V_1,\ V_2,\ V_3,\ V_4,\ V_5,\ V_6,\ V_7,\ V_8,\ V_9,\ V_{10},\ V_{11},\ V_{12},\ V_{13}]^T. \tag{A.3}$$

For the first line $i = 1$, rewrite the continuity equation (2.24), in the form:

$$L_{1,3} * V_3 + L_{1,5} * V_5 = \alpha F_{1,1} * V_1, \tag{A.4}$$

with

$$L_{1,3} = Dy,$$

$$L_{1,5} = i\beta\mathbf{I}$$

and

$$F_{1,1} = -i\mathbf{I}.$$

It is worth noting that each element of the matrices L and F are square matrices with dimension n, with n being the number of Chebyshev modes used to approximate the derivatives by polynomials; Dy is the Chebyshev matrix for the first derivative, and $Dy2$ is the Chebyshev matrix for the second derivative. All other elements for both matrices in this row are null.

The second line, $i = 2$, is one of the lines included in the system so that the matrices L and F are square, so in that line, we have:

$$L_{2,2} * V_2 = \alpha F_{2,1} * V_1, \tag{A.5}$$

with $L_{2,2} = F_{2,1} = \mathbf{I}$.

For $i = 3$, rewrite the quantity equation of motion in the x direction (2.25), in the form

$$\begin{aligned} L_{3,1} * V_1 + L_{3,3} * V_3 + L_{3,9} * V_9 + L_{3,10} * V_{10} = \alpha \left(F_{3,1} * V_1 + F_{3,2} * V_2 + \right. \\ \left. + F_{3,7} * V_7 + F_{3,8} * V_8\right), \end{aligned} \tag{A.6}$$

with

$$L_{3,1} = -i\omega\mathbf{I} - \frac{\beta_{nn}}{Re}(Dy2 - \beta^2\mathbf{I}),$$

$$L_{3,3} = \frac{dU}{dy},$$

$$L_{3,9} = -Dy,$$

$$L_{3,10} = -i\beta\mathbf{I},$$

$$F_{3,1} = -iU,$$

$$F_{3,2} = -\frac{\beta_{nn}}{Re}\mathbf{I},$$

$$F_{3,7} = -i\mathbf{I},$$

and

$$F_{3,8} = i\mathbf{I}.$$

For $i = 4$, the procedure is the same as for the row $i = 2$,

$$L_{4,4} * V_4 = \alpha F_{4,3} * V_3, \tag{A.7}$$

with $L_{4,4} = F_{4,3} = \mathbf{I}$.

For $i = 5$, rewrite the quantity equation of motion in the y direction (2.26), of the form:

$$L_{5,3} * V_3 + L_{5,7} * V_7 + L_{5,11} * V_{11} + L_{5,12} * V_{12} = \alpha \left(F_{5,3} * V_3 + F_{5,4} * V_4 + F_{5,9} * V_9 \right), \quad \text{(A.8)}$$

with

$$L_{5,3} = -i\omega\mathbf{I} - \frac{\beta_{nn}}{Re}(Dy2 - \beta^2\mathbf{I}),$$
$$L_{5,7} = Dy,$$
$$L_{5,11} = -Dy,$$
$$L_{5,12} = -i\beta\mathbf{I},$$
$$F_{5,3} = -iU,$$
$$F_{5,4} = -\frac{\beta_{nn}}{Re}\mathbf{I},$$
$$F_{5,9} = i\mathbf{I}.$$

For $i = 6$, the procedure is the same as for the rows $i = 2$ and $i = 4$,

$$L_{6,6} * V_6 = \alpha F_{6,5} * V_5, \quad \text{(A.9)}$$

with $L_{6,6} = F_{6,5} = \mathbf{I}$.

For the line $i = 7$, rewrite the quantity equation of motion in the z direction (2.27), of the form

$$L_{7,5} * V_5 + L_{7,7} * V_7 + L_{7,12} * V_{12} + L_{7,13} * V_{13} = \alpha \left(F_{7,5} * V_5 + F_{7,6} * V_6 + F_{7,10} * V_{10} \right), \quad \text{(A.10)}$$

with

$$L_{7,5} = -i\omega\mathbf{I} - \frac{\beta_{nn}}{Re}(Dy2 - \beta^2\mathbf{I}),$$
$$L_{7,7} = i\beta\mathbf{I},$$
$$L_{7,12} = -Dy,$$
$$L_{7,13} = -i\beta\mathbf{I},$$
$$F_{7,5} = -iU,$$
$$F_{7,6} = -\frac{\beta_{nn}}{Re}\mathbf{I},$$
$$F_{7,10} = i\mathbf{I}.$$

For $i = 8$, rewrite the constitutive equation for the tensor T_{xx} (2.28), of the form

$$\begin{aligned} L_{8,1} * V_1 + L_{8,3} * V_3 + L_{8,8} * V_8 + L_{8,9} * V_9 + L_{8,11} * V_{11} + L_{8,13} * V_{13} = \\ = \alpha \left(F_{8,1} * V_1 + F_{8,3} * V_3 + F_{8,8} * V_8 \right), \end{aligned} \quad \text{(A.11)}$$

with

$$L_{8,1} = -2WiTb_{xy}Dy + \xi WiTb_{xy}Dy,$$

$$L_{8,3} = Wi\frac{dTb_{xx}}{dy},$$

$$L_{8,8} = \mathbf{I} + \frac{\varepsilon ReWi}{(1-\beta_{nn})}(2Tb_{xx} + Tb_{yy}) - i\omega Wi\mathbf{I} + 2\frac{ReWi\alpha_G}{(1-\beta_{nn})}Tb_{xx},$$

$$L_{8,9} = -2Wi\frac{dU}{dy} + \xi Wi\frac{dU}{dy} + 2\frac{ReWi\alpha_G}{(1-\beta_{nn})}Tb_{xy},$$

$$L_{8,11} = \frac{\varepsilon ReWi}{(1-\beta_{nn})}Tb_{xx},$$

$$L_{8,13} = \frac{\varepsilon ReWi}{(1-\beta_{nn})}Tb_{xx},$$

$$F_{8,1} = 2iWiTb_{xx} - 2i\xi WiTb_{xx} + 2i\frac{(1-\beta_{nn})}{Re}\mathbf{I},$$

$$F_{8,3} = -i\xi WiTb_{xy},$$

$$F_{8,8} = -iWiU.$$

For $i = 9$, rewrite the constitutive equation for the tensor T_{xy} (2.29), of the form

$$\begin{aligned} L_{9,1} * V_1 + L_{9,3} * V_3 + L_{9,5} * V_5 + L_{9,8} * V_8 + L_{9,9} * V_9 + L_{9,11} * V_{11} + L_{9,13} * V_{13} = \\ = \alpha\left(F_{9,1} * V_1 + F_{9,3} * V_3 + F_{9,9} * V_9\right), \end{aligned} \tag{A.12}$$

with

$$L_{9,1} = -WiTb_{yy}Dy + \frac{1}{2}\xi Wi(Tb_{xx} + Tb_{yy})Dy - \frac{(1-\beta_{nn})}{Re}Dy,$$

$$L_{9,3} = Wi\frac{dTb_{xy}}{dy} + \xi WiTb_{xy}Dy,$$

$$L_{9,5} = i\beta WiTb_{xy},$$

$$L_{9,8} = \frac{\varepsilon ReWi}{(1-\beta_{nn})}Tb_{xy} + \frac{1}{2}\xi Wi\frac{dU}{dy} + \frac{ReWi\alpha_G}{(1-\beta_{nn})}Tb_{xy},$$

$$L_{9,9} = \mathbf{I} + \frac{\varepsilon ReWi}{(1-\beta_{nn})}(Tb_{xx} + Tb_{yy}) - i\omega Wi\mathbf{I} + \frac{ReWi\alpha_G}{(1-\beta_{nn})}(Tb_{xx} + Tb_{yy}),$$

$$L_{9,11} = \frac{\varepsilon ReWi}{(1-\beta_{nn})}Tb_{xy} - Wi\frac{dU}{dy} + \frac{1}{2}\xi Wi\frac{dU}{dy} + \frac{ReWi\alpha_G}{(1-\beta_{nn})}Tb_{xy},$$

$$L_{9,13} = \frac{\varepsilon ReWi}{(1-\beta_{nn})}Tb_{xy},$$

$$F_{9,1} = -i\xi WiTb_{xy},$$

$$F_{9,3} = iWiTb_{xx} - \frac{1}{2}i\xi Wi(Tb_{xx} + Tb_{yy}) + i\frac{(1-\beta_{nn})}{Re}\mathbf{I},$$

$$F_{9,9} = -iWiU.$$

For $i = 10$, rewrite the constitutive equation for the tensor T_{xz} (2.30), of the form

$$\begin{aligned} L_{10,1} * V_1 + L_{10,3} * V_3 + L_{10,5} * V_5 + L_{10,10} * V_{10} + L_{10,12} * V_{12} = \\ = \alpha\left(F_{10,5} * V_5 + F_{10,10} * V_{10}\right), \end{aligned} \tag{A.13}$$

with

$$L_{10,1} = \frac{1}{2} i\beta\xi WiTb_{xx} - i\beta\frac{(1-\beta_{nn})}{Re}\mathbf{I},$$

$$L_{10,3} = \frac{1}{2} i\beta\xi WiTb_{xy},$$

$$L_{10,5} = -WiTb_{xy}Dy + \frac{1}{2}\xi WiTb_{xy}Dy,$$

$$L_{10,10} = \mathbf{I} + \frac{\varepsilon ReWi}{(1-\beta_{nn})}(Tb_{xx} + Tb_{yy}) - i\omega Wi\mathbf{I} + \frac{ReWi\alpha_G}{(1-\beta_{nn})}Tb_{xx},$$

$$L_{10,12} = -Wi\frac{dU}{dy} + \frac{1}{2}\xi Wi\frac{dU}{dy} + \frac{ReWi\alpha_G}{(1-\beta_{nn})}Tb_{xy},$$

$$F_{10,5} = iWiTb_{xx} - \frac{1}{2} i\xi WiTb_{xx} + i\frac{(1-\beta_{nn})}{Re}\mathbf{I},$$

$$F_{10,10} = -iWiU.$$

For $i = 11$, rewrite the constitutive equation for the tensor T_{yy} (2.31), of the form

$$\begin{aligned} L_{11,1} * V_1 + L_{11,3} * V_3 + L_{11,8} * V_8 + L_{11,9} * V_9 + L_{11,11} * V_{11} + L_{11,13} * V_{13} = \\ = \alpha\left(F_{11,3} * V_3 + F_{11,11} * V_{11}\right), \end{aligned} \tag{A.14}$$

with

$$L_{11,1} = \xi WiTb_{xy}Dy,$$

$$L_{11,3} = Wi\frac{dTb_{yy}}{dy} - 2WiTb_{yy}Dy + 2\xi WiTb_{yy}Dy - 2\frac{(1-\beta_{nn})}{Re}Dy,$$

$$L_{11,8} = \frac{\varepsilon ReWi}{(1-\beta_{nn})}Tb_{yy},$$

$$L_{11,9} = \xi Wi\frac{dU}{dy} + 2\frac{ReWi\alpha_G}{(1-\beta_{nn})}Tb_{xy},$$

$$L_{11,11} = \mathbf{I} + \frac{\varepsilon ReWi}{(1-\beta_{nn})}(Tb_{xx} + 2Tb_{yy}) - i\omega Wi\mathbf{I} + 2\frac{ReWi\alpha_G}{(1-\beta_{nn})}Tb_{yy},$$

$$L_{11,13} = \frac{\varepsilon ReWi}{(1-\beta_{nn})}Tb_{yy},$$

$$F_{11,3} = 2iWiTb_{xy} - i\xi WiTb_{xy},$$

$$F_{11,11} = -iWiU.$$

For $i = 12$, rewrite the constitutive equation for the tensor T_{yz} (2.32), of the form

$$\begin{aligned} L_{12,1} * V_1 + L_{12,3} * V_3 + L_{12,5} * V_5 + L_{12,10} * V_{10} + L_{12,12} * V_{12} = \\ = \alpha\left(F_{12,5} * V_5 + F_{12,12} * V_{12}\right), \end{aligned} \tag{A.15}$$

with

$$L_{12,1} = \frac{1}{2} i\beta\xi WiTb_{xy},$$

$$L_{12,3} = \frac{1}{2} i\beta\xi WiTb_{yy} - i\beta\frac{(1-\beta_{nn})}{Re}\mathbf{I},$$

$$L_{12,5} = -WiTb_{yy}Dy + \frac{1}{2}\xi WiTb_{yy}Dy - \frac{(1-\beta_{nn})}{Re}Dy,$$

$$L_{12,10} = \frac{1}{2}\xi Wi\frac{dU}{dy} + \frac{ReWi\alpha_G}{(1-\beta_{nn})}Tb_{xy},$$

$$L_{12,12} = \mathbf{I} + \frac{\varepsilon ReWi}{(1-\beta_{nn})}(Tb_{xx} + Tb_{yy}) - i\omega Wi\mathbf{I} + \frac{ReWi\alpha_G}{(1-\beta_{nn})}Tb_{yy},$$

$$F_{12,5} = iWiTb_{xy} - \frac{1}{2}i\xi WiTb_{xy},$$

$$F_{12,12} = -iWiU.$$

And finally, for the line $i = 13$, we rewrite the constitutive equation for the tensor T_{zz} (2.33), of the form

$$L_{13,5} * V_5 + L_{13,13} * V_{13} = \alpha F_{13,13} * V_{13}, \tag{A.16}$$

with

$$L_{13,5} = -2i\beta\frac{(1-\beta_{nn})}{Re}\mathbf{I},$$

$$L_{13,13} = \mathbf{I} + \frac{\varepsilon ReWi}{(1-\beta_{nn})}(Tb_{xx} + Tb_{yy}) - i\omega Wi\mathbf{I},$$

$$F_{13,13} = -iWiU.$$


ICMC
USP
SÃO CARLOS